Attachment 1
NRC3-13-0015
(191 pages)

FSAR Markups

The following markup represents how DTE Electric intends to reflect this RAI response in the next submittal of the Fermi 3 COLA. However, the same COLA content may be impacted by responses to other COLA RAIs, other COLA changes, plant design changes, editorial or typographical corrections, etc. As a result, the final COLA content that appears in a future submittal may be different than presented here.

including extensive service to the Atomic Energy Commission in the development of facilities at Los Alamos, New Mexico. More recent activities include the development activities for other COLAs, the Advanced Boiling Water Reactor (AWBR) Design Certification Program, and the Department of Energy's 2010 initiative for the deployment of new nuclear plants in the United States. Various subcontractors are supporting Black & Veatch, including:

1.4.3.1 Professional Service Industries, Inc. (PSI)

PSI performed laboratory testing in support of Fermi 3 site specific evaluations in Chapter 2 and the Environmental Report. This effort included laboratory testing of rock and soil materials and water quality.

, developed the foundation input response spectra in support of Subsection 3.7.1, and developed inputs for soil-structure interaction (SSI) analyses in support of Subsection 3.7.2.

1.4.3.2 Boart Longyear

Boart Longyear performed geotechnical field investigations in support of Chapter 2. That effort included performing standard penetration tests; obtaining core samples and rock cores; performing cone penetrometer tests; supporting down-hole seismic tests and laboratory tests of soil and rock samples; installing ground water observation wells; and preparing a data report.

AMEC/

1.4.3.3 Geomatrix

Geomatrix Inc. performed probabilistic seismic hazard assessments and related sensitivity analyses in support of Chapter 2. These assignments included sensitivity analyses of seismic source parameters and updated ground motion attenuation relationships, development of updated Safe Shutdown Earthquake (SSE) ground motion values, and preparation of the related sections.

Other subcontractors may be added as needed.

1.4.4 Other Contractors

In addition to the major contractors listed above, contractual relationships may be established with specialized consultants to assist in developing the COLA as the need arises.

1.5 Requirements for Further Technical Information

This section of the referenced DCD is incorporated by reference with no departures or supplements.

1.8 Interfaces with Standard Design

This section of the referenced DCD is incorporated by reference with the following departures and/or supplements.

1.8.2 Identification of Balance of Plant Interfaces

Add the following paragraph after the first paragraph of this section.

STD CDI

The significant interface requirements for those systems that are beyond the scope of the DCD are identified in DCD Tier 1.

Delete the second sentence of the second paragraph of this section.

EF3 SUP 1.8-7

1.8.2.8 Independent Spent Fuel Storage Installation

Replace this section with the following.

No Fermi 3 ISFSI is currently planned. Any future Fermi 3 ISFSI will be located considering the impacts of external hazards as required by the associated 10 CFR 72 license for the Fermi 3 ISFSI.

EF3 SUP 1.8-1

1.8.3 Verification of Site Parameters

Chapter 2.0 provides information demonstrating that the site characteristics fall within the ESBWR site parameters specified in the referenced certified design.

, except for the "minimum shear wave velocity" in Table 2.0-1

EF3 SUP 1.8-2

1.8.4 COL Information Items and Permit Conditions

Section 1.10 identifies specific FSAR sections that address the COL Information items from the referenced certified design, and COL Action Items.

Table 1.8-202 Conceptual Design Information (CDI) (Sheet 1 of 2)

[EF3 SUP 1.8-5]

Item in DCD	CDI in DCD adopted as actual design	CDI in DCD replaced with actual design	Evaluation	FSAR Section
1.1.2.1 ESBWR Standard Plant Scope Figure 1.1-1 ESBWR Standard Plant General Site Plan		X	Site plan general site plan provided	1.1.2.1 Figure 2.1-204
1.2.2.11.4 Main Turbine	X		Conceptual turbine type selected as site specific design	1.2.2.11.4
1.2.2.11.7 Main Condenser	X		Conceptual condenser type selected as site specific design	1.2.2.11.7
1.2.2.12.13 Hydrogen Water Chemistry Table 3.2-1 P73 Note 9.3.9 Hydrogen Water Chemistry		X	Hydrogen water chemistry option utilized	1.2.2.12.13 9.3.9
1.2.2.12.15 Zinc Injection System Table 3.2-1 P74 Note 9.3.11 Zinc Injection System		X	Zinc Injection system not utilized	1.2.2.12.15 9.3.11
1.2.2.12.16 Freeze Protection		X	Freeze protection incorporated for external tanks and piping that may freeze during winter weather	1.2.2.12.16
1.2.2.16.10 Other Building Structures		X	Site-specific buildings specified	1.2.2.16.10
1.8.2 Identification of BOP Interfaces	X		Not applicable	
Appendix 3A Seismic Soil-Structure Interaction Analysis		X	Site-specific geotechnical data described in Chapter 2	Appendix 3A Chapter 2
Appendix 3A.2 ESBWR Standard Site Plan		X	Site-specific general site plan provided	Appendix 3A Figure 2.1-201
9.2.1 Plant Service Water Table 9.2-2 Figure 9.2-1		X	Site-specific system description and design characteristics described	9.2.1 Table 9.2-201 Figure 9.2-205
9.2.3 Makeup Water System Table 9.2-9		X	Site-specific system description and design characteristics described	9.2.3 Table 9.2-202

and Subsection 3.7.1, and site-specific SSI analyses described in Subsection 3.7.1, Subsection 3.7.2, and Subsection 3.8.5

3.7.1, 3.7.2, and 3.8.5

Regulatory Guide 1.206

Table 1.9-203 evaluates conformance with the FSAR content guidance in RG 1.206. Where necessary, the table identifies the FSAR section where the required information is provided. In the table, the term "Conforms" means that the information called for in RG 1.206 is either: 1) already addressed in the DCD; or 2) addressed by adding new information beyond that contained in the DCD. The term "Not applicable" means that the information called for in RG 1.206 does not apply to the ESBWR or Fermi 3.

Table 1.9-203 evaluates conformance with RG 1.206, Section C.III.1 , "Information Needed for a Combined License Application Referencing a Certified Design." Section C.I, "Standard Format and Content of Combined License Applications for Nuclear Power Plants-Light-Water Reactor Edition," were also evaluated, as applicable, if portions of these sections were referenced or identified in RG 1.206, Section C.III.1 .

EF3 SUP 1.9-1

Industrial Codes and Standards

Table 1.9-204 identifies the Industrial Codes and Standards that are applicable to those portions of the Fermi 3 design that are beyond the scope of the DCD, and to the operational aspects of the facility.

1.9.3 Applicability of Experience Information

Add the following after the first sentence of the section.

, NUREG/CP, NUREG/GR,

EF3 SUP 1.9-2

Table 1.9-205 lists NUREG and NUREG/CR reports cited in the FSAR.

Add the following paragraph at the end of this section.

Table 1.9-205 addresses operational experience information, as described in applicable NUREG reports, for those portions of the Fermi 3 design and operation that are beyond the scope of the DCD. The comment column of Table 1.9-205 includes a reference to the applicable FSAR section that provides further discussion of the operational experience.

Table 1.9-201 Conformance with Standard Review Plan (Sheet 2 of 48) [EF3 COL 1.9-3-A]

SRP Section	Title	Rev	Date	Specific Acceptance Criteria	Evaluation
2.4.2	Floods	Rev. 4	Mar-07	II.1, II.2, II.3, II.4, II.5, II.6, II.7, II.8, II.9, II.10	Conforms
2.4.3	Probable Maximum Flood (PMF) on Streams and Rivers	Rev. 4	Mar-07	II.1, II.2, II.3	Conforms
2.4.4	Potential Dam Failures	Rev. 3	Mar-07	II.1, II.2, II.3, II.4, II.5, II.6, II.7	Conforms
2.4.5	Probable Maximum Surge and Seiche Flooding	Rev. 3	Mar-07	II.1, II.2, II.3, II.4, II.5, II.6	Conforms
2.4.6	Probable Maximum Tsunami Hazards	Rev. 3	Mar-07	II.1, II.2, II.3, II.4, II.5, II.6, II.7, II.8	Conforms
2.4.7	Ice Effects	Rev. 3	Mar-07	II.1, II.2, II.3, II.4, II.5	Conforms
2.4.8	Cooling Water Canals and Reservoirs	Rev. 3	Mar-07	II.1, II.2, II.3, II.4	Conforms
2.4.9	Channel Diversions	Rev. 3	Mar-07	II.1, II.2, II.3, II.4, II.5, II.6, II.7	Conforms
2.4.10	Flooding Protection Requirements	Rev. 3	Mar-07	II.1, II.2, II.3, II.4	Conforms
2.4.11	Low Water Considerations	Rev. 3	Mar-07	II.1, II.2, II.3, II.4, II.5	Conforms
2.4.12	Groundwater	Rev. 3	Mar-07	II.1, II.2, II.3, II.4, II.5	Conforms
2.4.13	Accidental Releases of Radioactive Liquid Effluents in Ground and Surface Waters	Rev. 3	Mar-07	II.1, II.2, II.3, II.4, II.5	Conforms. A tank rupture analysis was not performed since special design features were incorporated to mitigate the consequences of failures.
2.4.14	Technical Specifications and Emergency Operation Requirements	Rev. 3	Mar-07	II.1, II.2, II.3, II.4, II.5	Conforms
2.5.1	Basic Geologic and Seismic Information	Rev. 4	Mar-07	II.1, II.2	Conforms, except that NUREG-2115 is incorporated as the replacement for the Lawrence Livermore National Laboratory and the Electric Power Research Institute studies in the Central and Eastern United States.
2.5.2	Vibratory Ground Motion	Rev. 4	Mar-07	~~II.1, II.2, II.3, II.4, II.5, II.6~~ II.2	Conforms

All except II.2

Table 1.9-201 Conformance with Standard Review Plan (Sheet 4 of 48) [EF3 COL 1.9-3-A]

SRP Section	Title	Rev	Date	Specific Acceptance Criteria	Evaluation
3.5.3	Barrier Design Procedures	Rev. 3	Mar-07	II.1, II.2	Conforms
3.6.1	Plant Design for Protection Against Postulated Piping Failures in Fluid Systems Outside Containment	Rev. 3	Mar-07	II.1, II.2, II.3, II.4, II.5	Conforms
3.6.2	Determination of Rupture Locations and Dynamic Effects Associated with the Postulated Rupture of Piping	Rev. 2	Mar-07	II.1, II.2, II.3	Conforms
3.6.3	Leak-Before-Break Evaluation Procedures	Rev. 1	Mar-07	II.1, II.2	Not applicable. ESBWR design does not rely on a Leak Before Break Evaluation.
3.7.1	Seismic Design Parameters	Rev. 3	Mar-07	All except ~~II.1 and~~ II.4	Conforms except that the ESBWR is based on a single earthquake (SSE) design.
				~~II.1~~	~~Conforms with the exception of the statistical independence correlation coefficient specified in SRP 3.7.1.II Acceptance Criteria 1.B. Justification for the methodology used is described in Section 3.7.1.~~
				II.4	Conforms - supplemented by "Interim Staff Guidance on Seismic Issues Associated with High Frequency Ground Motion in Design Certification and Combined License Applications," ~~COL/DCISG-1~~, May 2008.
3.7.2	Seismic System Analysis	Rev. 3	Mar-07	II.1, II.2, II.3, II.4, II.5, II.6, II.7, II.8, II.9, II.10, II.11, II.12, II.13, II.14	Conforms

Supplemented by "Interim Staff Guidance on Ensuring Hazard-Consistent Seismic Input for Site Response and Soil Structure Interaction Analyses," DC/COL-ISG-017, March 2010.

DC/COL-ISG-1

Table 1.9-202 Conformance with Regulatory Guides (Sheet 22 of 26)
[EF3 COL 1.9-3-A]

RG Number	Title	Revision	Date	RG Position	Evaluation
1.201	Guidelines for Categorizing Structures, Systems, and Components in Nuclear Power Plants According to Their Safety Significance	Rev. 1	May-06	General	Not applicable
1.202	Standard Format and Content of Decommissioning Cost Estimates for Nuclear Power Reactors	Rev. 0	Feb-05	General	Not applicable. The RG provides guidance for submitting decommissioning cost estimates to NRC prior to license termination.
1.203	Transient and Accident Analysis Methods	Rev. 0	Dec-05	General	Conforms
1.204	Guidelines for Lightning Protection of Nuclear Power Plants	Rev. 0	Nov-05	General	Conforms. Operational program implementation is described in Section 13.4.
1.205	Risk-Informed, Performance-Based Fire Protection for Existing Light-Water Nuclear Power Plants	Rev. 0	May-06	General	Not applicable. Risk-informed, performance-based fire protection is not used.
1.206	Combined License Applications for Nuclear Power Plants (LWR Edition)	Rev. 0	Jun-07	General	See Table 1.9-203.
1.207	Guidelines for Evaluating Fatigue Analyses Incorporating the Life Reduction of Metal Components Due to the Effects of the Light-Water Reactor Environment for New Reactors	Rev. 0	Mar-07	General	Conforms
1.208	A Performance-Based Approach to Define the Site-Specific Earthquake Ground Motion	Rev. 0	Mar-07	All	Conforms, except that NUREG-2115 is incorporated as the replacement for the Lawrence Livermore National Laboratory and the Electric Power Research Institute studies in the Central and Eastern United States.

Table 1.9-204 Industrial Codes and Standards (Sheet 1 of 5) [EF3 SUP 1.9-1]

Code or Standard Number	Year	Title
American Concrete Institute (ACI)		
318-08	2008	Building Code Requirements for Structural Concrete and Commentary
349-01	2001	Code Requirements for Nuclear Safety-Related Concrete Structures
207.1R	2005 (Reapproved 2012)	Guide to Mass Concrete
207.2R	1995 (Reapproved 2002)	Report on Thermal and Volume Change Effects on Cracking of Mass Concrete
207.4R	2005 (Reapproved 2012)	Cooling and Insulating Systems for Mass Concrete
American Nuclear Society (ANS)		
2.8	1992	Determining Design Basis flooding at Power Reactor Sites an American
3.1	1993	Selection, Qualification, and Training of Personnel for Nuclear Power Plants
American National Standards Institute		
N323A	1997	Radiation Protection Instrumentation Test and Calibration, Portable Survey Instruments
N323D	2002	Installed Radiation Protection Instrumentation
B30.2	2001	Overhead and Gantry Cranes
American Society of Civil Engineers (ASCE)		
ASCE 43-05	2005	Seismic Design Criteria for Structures, Systems, and Components in Nuclear Facilities
ASCE SEI/ASCE 7-05	2005	Minimum Design Loads for Buildings and other Structures
ASCE Practice No. 70	1990	Evapotranspiration and Irrigation Water Requirements
American Society Heating, Refrigerating, and Air-Conditioning (ASHRAE)		
ASHRAE Handbook	2005	American Society Heating, Refrigerating, and Air-Conditioning Engineers Handbook
American Society of Mechanical Engineers (ASME)		
NQA-1	1994	Quality Assurance Programs Requirements for Nuclear Facilities
Boiler and Pressure Vessel Code, Section IX	2007	Qualification Standard for Welding and Brazing Procedures, Welder, Brazers and Welding and Brazing Operators
OM Code		Code for the Operation and Maintenance of Nuclear Power Plants
ASCE 4-98	1998	Seismic Analysis of Safety-Related Nuclear Structures and Commentary

Table 1.9-205 NUREG Reports Cited (Sheet 1 of 2) [EF3 SUP 1.9-2]

NUREG No.	Issue Date	Title	Comment/Section Where Discussed
0016, Rev. 1	01/1979	Calculation of Releases of Radioactive Materials in Gaseous and Liquid Effluents from Boiling Water Reactors (BWRs)	12.2, Table 1.9-202 RG 1.111
0570	06/1979	Toxic Vapor Concentrations in the Control Room Following a Postulated Accidental Release	6.4
0612	07/1980	Control of Heavy Loads at Nuclear Power Plants	13.5, 9.1.5
0737	11/1980	Clarification of TMI Action Plan Requirements	12.5, 13.5, Appendix 14AA
0800	03/2007	Standard Review Plan for the Review of Safety Analysis Reports for Nuclear Power Plants	1.1, 2.0, 2.2, 2.3, 2.4, 2.5, 9.3, 11.5, Appendix 14AA
1437	05/1996	Generic Environmental Impact Statement for License Renewal of Nuclear Plants, U.S. Nuclear Regulatory Commission	12.2
1736	10/2001	Consolidated Guidance: 10 CFR Part 20 – Standards for Protection Against Radiation	1.9
1805	12/2004	Fire Dynamics Tools (FDTs) Quantitative Fire Hazard Analysis Methods for the U.S. Nuclear Regulatory Commission Fire Protection Inspection Program	2.2
0654/FEMA-REP-1	11/1980	Criteria for Preparation and Evaluation of Radiological Emergency Response Plans and Preparedness in Support of Nuclear Power Plants	1.9, Emergency Plan
0696	02/1981	Functional Criteria for Emergency Response Facilities", Final Report	Emergency Plan
0728	04/2005	NRC Incident Response Plan	Emergency Plan
0737, Sup 1	12/1982	Requirements for Emergency Response Capability	13.5, Emergency Plan
CR-1745	11/1980	Analysis of Techniques for Estimating Evacuation Times for Emergency Planning Zones,	Emergency Plan, ETE
CR-2650	10/1982	Allowable Shipment Frequencies for the Transport of Toxic Gases Near Nuclear Power Plants	2.2.3
CR-2858	11/82	PAVAN: An Atmospheric Dispersion Program for Evaluating Design Basis Accidental Releases of Radioactive Materials for Nuclear Power Stations	2.3.4
CR-2919	09/1982	XOQDDOQ: Computer Program for the Meteorological Evaluation of Routine Effluent Releases at Nuclear Power Stations	2.3.5, Appendix 2B
CR-3145	10/1992	Geophysical Investigations of the Western Ohio – Indiana Region	2.5.1, 2.5.2

Insert 1

Insert 2

NUREG No.	Issue Date	Title	Comment/Section Where Discussed
Insert 1			
1407	1991	Procedural and Submittal Guidance for the Individual Plant Examination of External Events (IPEEE) for Severe Accident Vulnerabilities	3.7.1
Insert 2			
CR-0098	1978	Development of Criteria for Seismic Review of Selected Nuclear Power Plants	3.7.1

Table 1.9-205 NUREG Reports Cited (Sheet 2 of 2) [EF3 SUP 1.9-2]

NUREG No.	Issue Date	Title	Comment/Section Where Discussed
CR-4013	04/1986	LADTAP II Technical Reference and User Guide	12.2
CR-4461	02/2007	Tornado Climatology of the United States	2.3
CR-4653	03/1987	GASPAR II Technical Reference and User Guide	12.2
CR-4831	03/1992	State of the Art in Evacuation Time Esitmate Studies for Nuclear Power Plants	Emergency Plan
CR-5250	1986	Seismic Hazard Characterization of 69 Nuclear Plant Sites East of the Rocky Mountains: Questionnaires," prepared by Lawrence Livermore National Laboratory	2.5.2
CR-5503	07/1999	Techniques for Identifying Faults and Determining Their Origins	2.5.3
CR-5512	10/1992	Residual Radioactive Contamination from Decomisioning	2.4
CR-6331	07/1997	Atmospheric Relative Concentrations in Building Wakes	2.3.4
CR-6372	04/1997	Recommendations for Probabilistic Seismic Hazard Analysis: Guidance on Uncertainty and Use of Experts	2.5.2
CR-6624	10/1992	Recommendations for Revision of Regulatory Guide 1.78	2.2
CR-6948	11/2007	Integrated Ground-Water Monitoring Strategy for NRC-Licensed Facilities and Sites: Logic, Strategic Approach and Discussion	2.4.12
CR-6728	10/2001	Technical Basis for Revision of Regulatory Guidance on Design Ground Motions: Hazard- and Risk-consistent Ground Motion Spectra Guidelines	2.5 , 3.7.1
CR-6863	01/2005	Development of Evacuation Time Estimate Studies for Nuclear Power Plants	Emergency Plan

Insert 3 →

Insert 4 →

NUREG No.	Issue Date	Title	Comment/Section Where Discussed
Insert 3			
CR-5347	1989	Recommendation for Resolution of Public Comments on USI A-40, "Seismic Design Criteria	3.7.1
Insert 4			
CR-6926	2007	Evaluation of the Seismic Design Criteria in ASCE/SEI Standard 43-05 for Application to Nuclear Power Plants	3.7.1

Table 1.10-201 Summary of FSAR Sections Where DCD COL Items Are Addressed (Sheet 2 of 7) [EF3 SUP 1.10-1]

Item No.	Subject/Description of Item	FSAR Section
2.0-16-A	Probable Maximum Surge and Seiche Flooding in Accordance with SRP 2.4.5	2.0 and 2.4.5
2.0-17-A	Probable Maximum Tsunami in Accordance with SRP 2.4.6	2.0 and 2.4.6
2.0-18-A	Ice Effects in Accordance with SRP 2.4.7	2.0 and 2.4.7
2.0-19-A	Cooling Water Canals and Reservoirs in Accordance with SRP 2.4.8	2.0 and 2.4.8
2.0-20-A	Channel Diversion in Accordance with SRP 2.4.9	2.0 and 2.4.9
2.0-21-A	Flooding Protection Requirements in Accordance with SRP 2.4.10	2.0 and 2.4.10
2.0-22-A	Cooling Water Supply in Accordance with SRP 2.4.11	2.0 and 2.4.11
2.0-23-A	Groundwater in Accordance with SRP 2.4.12	2.0 and 2.4.12
2.0-24-A	Accidental Releases of Liquid Effluents in Ground and Surface Waters in Accordance with SRP 2.4.13	2.0 and 2.4.13
2.0-25-A	Technical Specifications and Emergency Operation Requirements in Accordance with SRP 2.4.14	2.0 and 2.4.14
2.0-26-A	Basic Geologic and Seismic Information in Accordance with SRP 2.5.1	2.0 and 2.5.1
2.0-27-A	Vibratory Ground Motion in Accordance with SRP 2.5.2	2.0, 2.5.2, and 3.7.1 ~~2.0 and 2.5.2~~
2.0-28-A	Surface Faulting in Accordance with SRP 2.5.3	2.0 and 2.5.3
2.0-29-A	Stability of Subsurface Materials and Foundations in Accordance with SRP 2.5.4	2.0 and 2.5.4
2.0-30-A	Stability of Slopes in Accordance with SRP 2.5.5	2.0 and 2.5.5
2A.2-1-A	Confirmation of the ESBWR χ/Q Values	2.3.4.3 and 2A.2.4
2A.2-2-A	Confirmation of the Reactor Building χ/Q Values	2A.2.5
3.9.9-1-A	Reactor Internals Vibration Analysis, Measurement and Inspection Program	3.9.2.4
3.9.9-2-A	ASME Class 2 or 3 or Quality Group D Components with 60-Year Design Life	3.9.3.1
3.9.9-3-A	Inservice Testing Programs	3.9.6
3.9.9-4-A	Snubber Inspection and Test Program	3.9.3.7.1(3)e
3.10.4-1-A	Dynamic Qualification Report	3.10.1.4
3.11-1-A	Environmental Qualification Document (EQD)	3.11.4.4
4.3-1-A	Variances from Certified Design	4.3.3.1
4A-1-A	Variances from Certified Design	4A.1
5.2-1-A	Preservice and Inservice Inspection Program Description	5.2.4, 5.2.4.3.4, 5.2.4.6, 5.2.4.11, and 6.6

Table 2.0-201 Evaluation of Site/Design Parameters and Characteristics (Sheet 7 of 31) [EF3 COL 2.0-1-A]

Subject [16]	DCD Site Parameter Value[1][16]	Fermi 3 Site Characteristic	Evaluation
Ambient Design Temperature (continued)			
Maximum High Humidity Average Wet Bulb Globe Temperature Index for 0% Exceedance Maximum Wet Bulb Temperature Day	30.3°C (86.6°F)	28.78°C (83.8°F)	The Fermi 3 site characteristic value for Maximum High Humidity Average Wet Bulb Globe Temperature Index for 0% Exceedance Maximum Wet Bulb Temperature Day is 28.78°C (83.8°F). This value falls within (is less than) the DCD site parameter value for Maximum High Humidity Average Wet Bulb Globe Temperature Index for 0% Exceedance Maximum Wet Bulb Temperature Day.
Soil Properties			
Minimum Static Bearing Capacity[7]	Greater than or equal to the Maximum Static Bearing Demand.		
Maximum Static Bearing Demand:			
Reactor/Fuel Building	699 kPa (14,600 lbf/ft^2)	4,500 kPa (94,000 lbf/ft^2)	The Fermi 3 site characteristic value for allowable bearing capacity from Table 2.5.4-227 for the R/FB falls within (is greater than) the DCD site parameter value.
Control Building	292 kPa (6,100 lbf/ft^2)	14,029 kPa (293,000 lbf/ft^2)	The Fermi 3 site characteristic value for allowable bearing capacity from Table 2.5.4-227 for the CB falls within (is greater than) the DCD site parameter value.
Fire Water Service Complex	165 kPa (3450 lbf/ft^2)	1,532 kPa (32,000 lbf/ft^2)	The Fermi 3 site characteristic value for allowable bearing capacity from Table 2.5.4-227 for the FWSC falls within (is greater than) the DCD site parameter value.
Reactor/Fuel Building			
Soft	1,100 kPa (23,000 lbf/ft^2)	5,980 kPa (125,000 lbf/ft^2)	The Fermi 3 site characteristic value for allowable dynamic bearing capacity for the RB/FB structure is from Table 2.5.4-227 and falls within (is greater than) the DCD site parameter value.
Medium	2,700 kPa (56,400 lbf/ft^2)		
Hard	1,100 kPa (23,000 lbf/ft^2)		

In accordance with Note Number 16 of the DCD, Tier 2 Table 2.0-1, Fermi 3 site-specific soil structure interaction (SSI) analyses were performed for the RB/FB. The DCD site parameter value for dynamic bearing demand envelopes (is greater than) the SSI dynamic bearing demand for the RB/FB.

Table 2.0-201 Evaluation of Site/Design Parameters and Characteristics (Sheet 8 of 31) [EF3 COL 2.0-1-A]

Subject [16]	DCD Site Parameter Value[1][16]	Fermi 3 Site Characteristic	Evaluation
Soil Properties (continued)			
Minimum Dynamic Bearing Capacity[7]	Greater than or equal to the Maximum Dynamic Bearing Demand.		
Maximum Dynamic Bearing Demand (SSE & Static):			
Control Building			
Soft	500 kPa (10,500 lbf/ft^2)	18,700 kPa (391,000 lbf/ft^2)	The Fermi 3 site characteristic value for allowable dynamic bearing capacity for the CB structure is from Table 2.5.4-227 and falls within (is greater than) the DCD site parameter value .
Medium	2,200 kPa (46,000 lbf/ft^2)		
Hard	420 kPa (8,800 lbf/ft^2)		
Fire Water Service Complex (FWSC)			
Soft	460 kPa (9,600 lbf/ft^2)	2100 kPa (43,000 lbf/ft^2)	The Fermi 3 site characteristic value for allowable dynamic bearing capacity for the FWSC structure is from Table 2.5.4-227 and falls within (is greater than) the DCD site parameter value .
Medium	690 kPa (14,400 lbf/ft^2)		
Hard	1,200 kPa (25,100 lbf/ft^2)		

In accordance with Note Number 16 of the DCD, Tier 2 Table 2.0-1, Fermi 3 site-specific soil structure interaction (SSI) analyses were performed for the CB. The DCD site parameter value for dynamic bearing demand envelopes (is greater than) the SSI dynamic bearing demand for the CB.

The Fermi 3 site-specific SSI were performed with and without engineered granular backfill above the Bass Islands Group bedrock. Without engineered granular backfill above the Bass Islands Group bedrock, the SSI results are within (less than) the DCD requirements; therefore, the DCD site parameters for engineered granular backfill above the top of the Bass Islands Group bedrock do not apply.

Table 2.0-201 Evaluation of Site/Design Parameters and Characteristics (Sheet 9 of 31) [EF3 COL 2.0-1-A]

Subject [16]	DCD Site Parameter Value[1][16]	Fermi 3 Site Characteristic	Evaluation
Soil Properties (continued)			
Minimum Shear Wave Velocity[8]	300 m/s (1000 ft/s)	Value for supporting material for each Seismic Category I structure; RB/FB, CB, and FWSC greater than 1,000 ft/sec Value for surrounding material for each Seismic Category I structure: – Below top of bedrock – greater than 1,000 ft.sec – Above top of bedrock – neglected	In accordance with Note Number 16 of the Referenced DCD, Tier 2 Table 2.0-1, Fermi 3 site-specific soil structure interaction (SSI) analyses were performed for the RB/FB and CB. ~~In the Fermi 3 site-specific SSI, the engineered granular backfill above the top of the bedrock was neglected; therefore, the Reference DCD site parameter for backfill above the top of the bedrock does not apply.~~ Fill concrete is used as backfill below the top of bedrock surrounding the RB/FB and CB, and below the FWSC to the top of bedrock. Fill concrete and supporting bedrock meet the DCD requirement. For supporting foundation material the shear wave velocity for each structure falls within (is greater than) the DCD site parameter value. As shown in Figure 2.5.4-215 and Figure 2.5.4-216, the RB/FB, CB, and FWSC foundations are founded on uniform material. Therefore, the ratio of the largest of the smallest shear wave velocity over each mat foundation level does not exceed 1.7.
Liquefaction Potential			
Seismic Category I structures	None under footprint of Seismic Category I structures resulting from site-specific SSE	None at site-specific SSE under Seismic Category I structures	The Fermi 3 Category I structures are founded on bedrock or fill concrete and there is no potential for liquefaction under Fermi 3 Seismic Category I structures at the site-specific SSE ground motion.
Other than Seismic Category I structures	See Note (14)	See Evaluation column	Note (14) in DCD Table 2.0-1 identifies a requirement to address liquefaction potential under other than Seismic Category I structures. ~~S~~ubsection 2.5.4.8 provides the results of the analysis for the glacial till at the Fermi 3 site and addresses potential liquefaction under other than Seismic Category I structures. Based on the analysis provided, the glacial till ~~is~~ are not susceptible to liquefaction. and II
Angle of Internal Friction (in-situ and backfill)	≥35 degrees	≥35 degrees	The Fermi 3 site characteristic value for angle of internal friction is provided in Subsection 2.5.4.10 and falls within (is the same as) the DCD site parameter value.

engineered granular backfill and

Backfill below Seismic Category II structures from the base of the foundation to the top of bedrock is fill concrete; therefore, liquefaction analysis for soil below Seismic Category II structures is not necessary.

Table 2.0-201 Evaluation of Site/Design Parameters and Characteristics (Sheet 12 of 31) [EF3 COL 2.0-1-A]

Subject [16]	DCD Site Parameter Value[1][16]	Fermi 3 Site Characteristic	Evaluation
Seismology (continued)			
		~~See Figure 2.5.2-289 through Figure 2.5.2-291~~	The Fermi 3 site characteristic values are identified as the foundation input response spectra (FIRS). The CB FIRS are shown in Figure ~~2.5.2-290~~. The RB/FB FIRS are shown in Figure ~~2.5.2-289~~. The FWSC FIRS are shown in Figure ~~2.5.2-291~~. The comparisons of the DCD site parameter (CSDRS for the CB and RB/FB) and Fermi 3 site characteristic values (FIRS for the CB and RB/FB) are provided in Figure 2.0-201 ~~for the horizontal spectra~~ and ~~in~~ Figure 2.0-202 ~~for the vertical spectra~~. These comparisons demonstrate that the Fermi 3 site characteristic values fall within (are less than) the values established by the DCD site parameters. The comparisons of the DCD site parameter (CSDRS for the FWSC) and Fermi 3 site characteristic values (FIRS for the FWSC) are provided in Figure 2.0-203 ~~for the horizontal spectra and in Figure 2.0-204 for the vertical spectra~~. These comparisons demonstrate that the Fermi 3 site characteristic values fall within (are less than) the values established by the DCD site parameters.
Hazards in Site Vicinity			
Site Proximity Missiles and Aircraft	< about 10^{-7} per year (for site proximity missile hazards)	No site proximity missile hazards identified	The Fermi 3 site characteristic value for site proximity missiles value is that there are no site proximity missile sources identified. As provided in Subsection 2.2.1, there are no missile sources identified in the site vicinity and this value falls within (is less than) the DCD site parameter value.
	< about 10^{-7} per year (for aircraft hazards)	Annual aircraft crash probability of < about 1×10^{-7} (includes civil and military aircraft)	The Fermi 3 site characteristic value for total probability per year of a civil or military aircraft crashing was estimated per NUREG-0800 as shown in Subsection 2.2.3.1.3 and the total accident probability falls within (is the same as) the DCD site parameter value except as noted for Mills Field in Subsection 2.2.3.1.3.1.
Volcanic Activity	None	No volcanic activity at the site	The Fermi 3 site characteristic value for volcanic activity is that there is no evidence of non-tectonic deformation at the site, such as volcanic intrusion, as presented in Subsection 2.5.3. The Fermi 3 site characteristic value falls within (is the same as) the DCD site parameter value.
Toxic Gases	None*		

See Figure 3.7.1-228, Figure 3.7.1-229, and Figure 3.7.1-238

3.7.1-228

enhanced Soil Column Outcrop Response (SCOR)

3.7.1-229

enhanced SCOR

3.7.1-238

enhanced SCOR

Figure 2.0-201 **Comparison of Horizontal CSDRS with the Unit 3 FIRS for the RB/FB and CB** [EF3 COL 2.0-1-A]

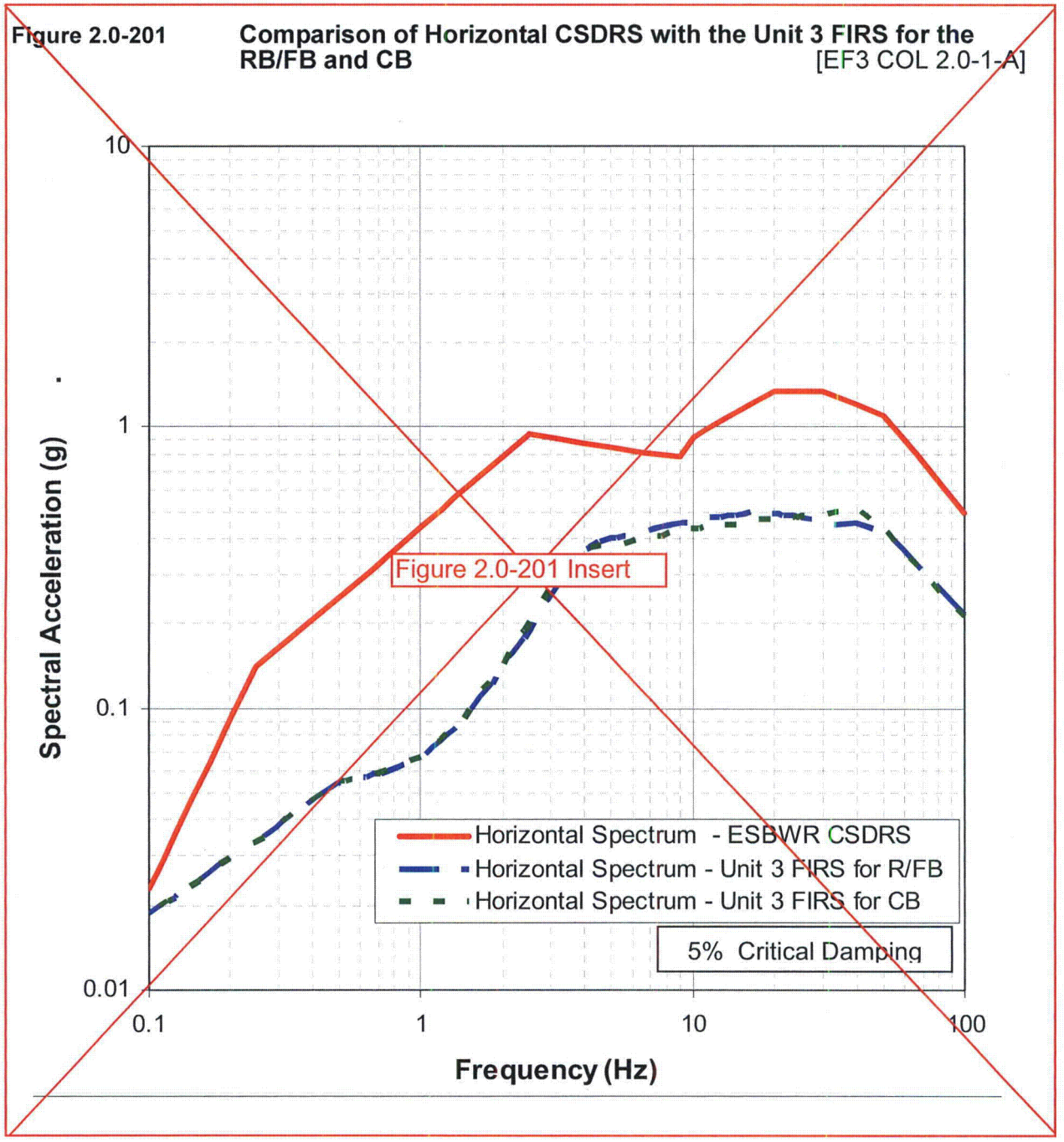

Figure 2.0-201 Insert

Figure 2.0-201 Horizontal and Vertical RB/FB Enhanced SCOR FIRS and CSDRS [5 Percent Damping] (FIRS are developed in Subsection 3.7.1)

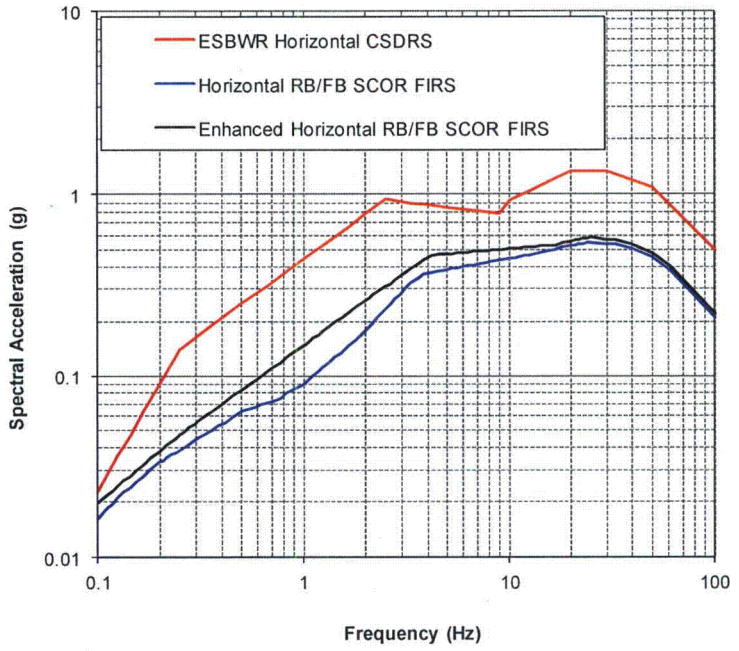

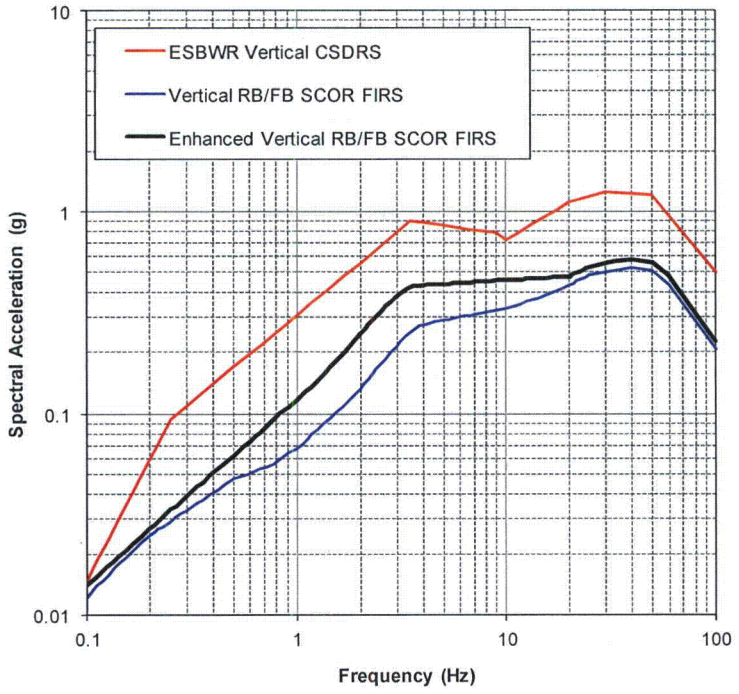

Figure 2.0-202 **Comparison of Vertical CSDRS with the Unit 3 FIRS for the RB/FB and CB** [EF3 COL 2.0-1-A]

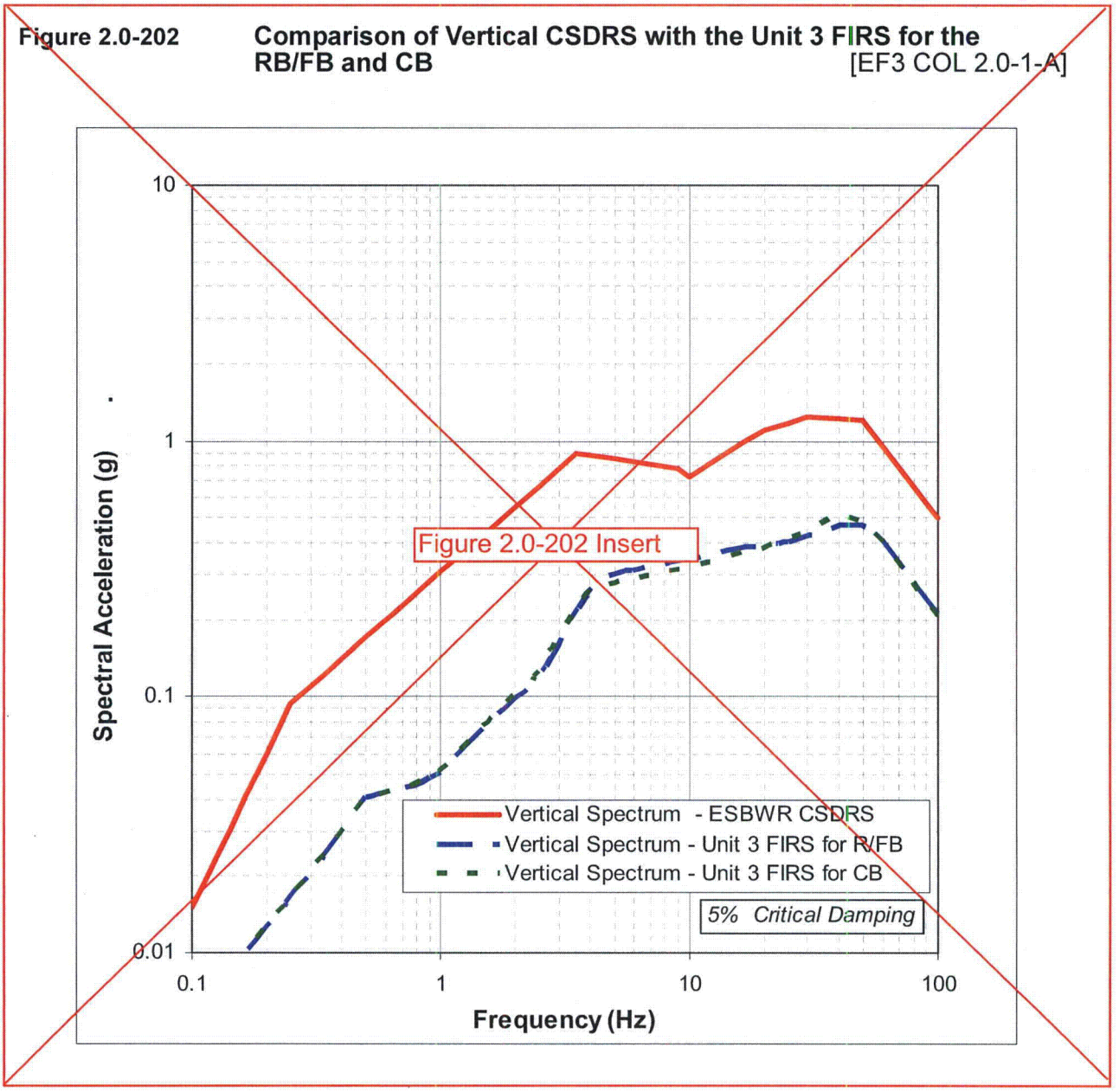

Figure 2.0-202 Insert

Figure 2.0-202 Horizontal and Vertical CB Enhanced SCOR FIRS and CSDRS [5 Percent Damping]
(FIRS are developed in Subsection 3.7.1)

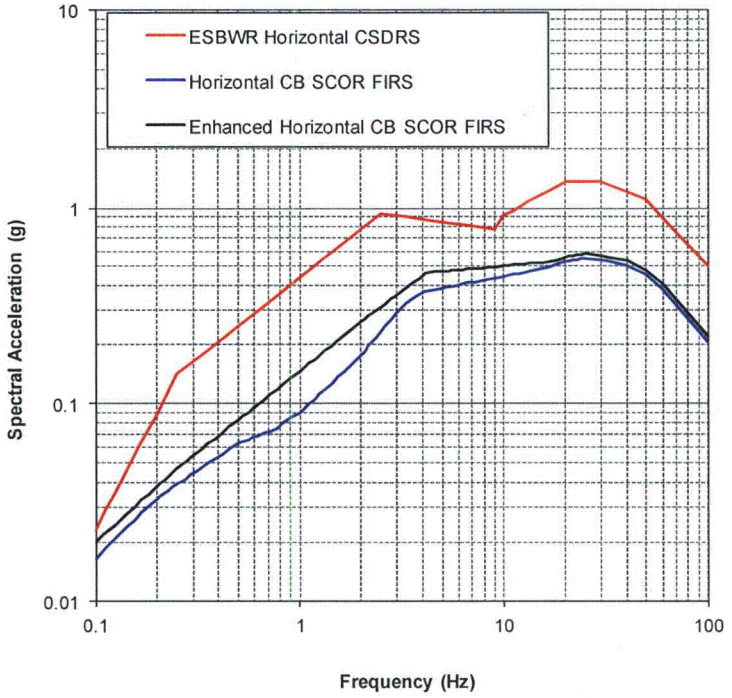

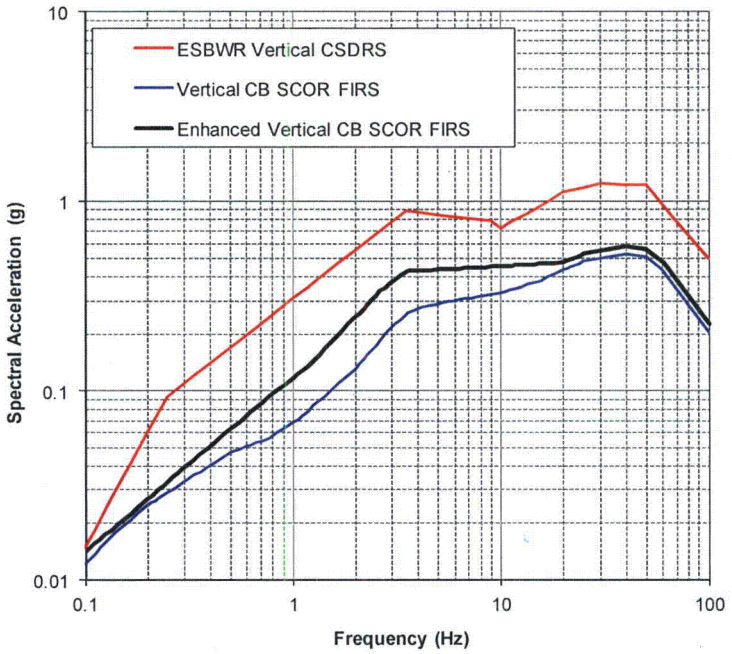

Figure 2.0-203 **Comparison of Horizontal CSDRS with the Unit 3 FIRS for the FWSC** [EF3 COL 2.0-1-A]

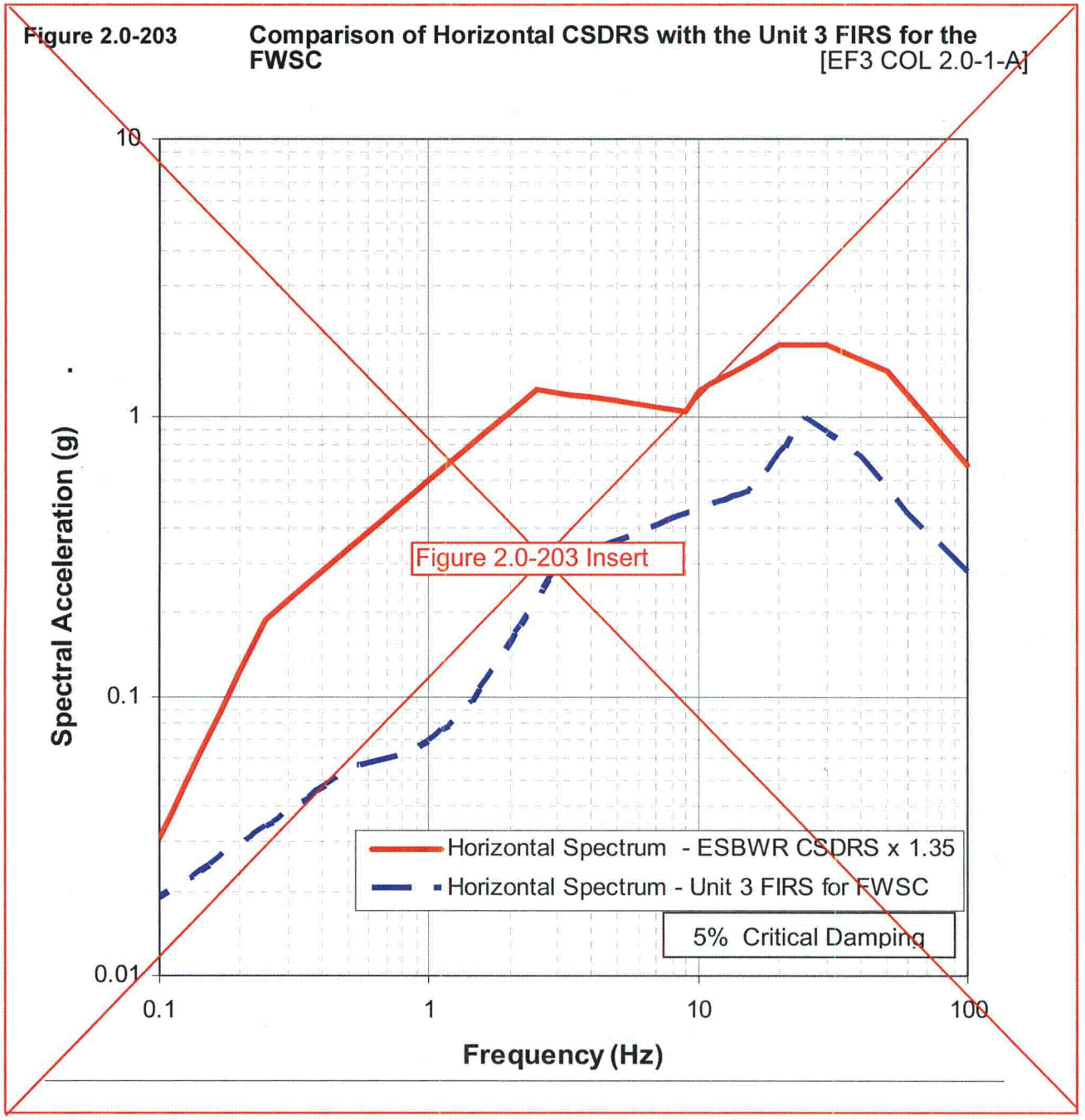

Figure 2.0-203 Insert

Figure 2.0-203 Horizontal and Vertical FWSC FIRS and 1.35 Times the CSDRS [5 Percent Damping] (FIRS are developed in Subsection 3.7.1)

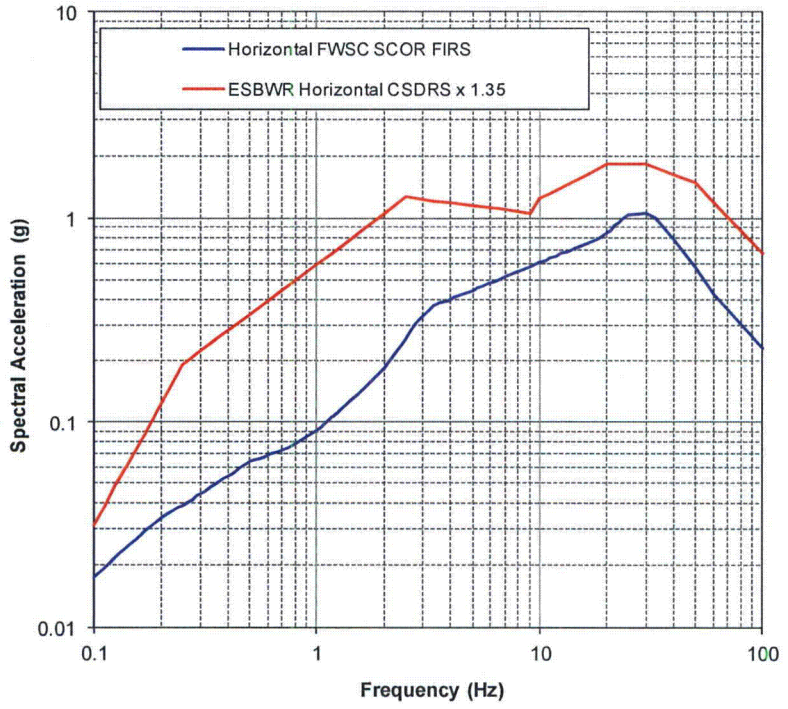

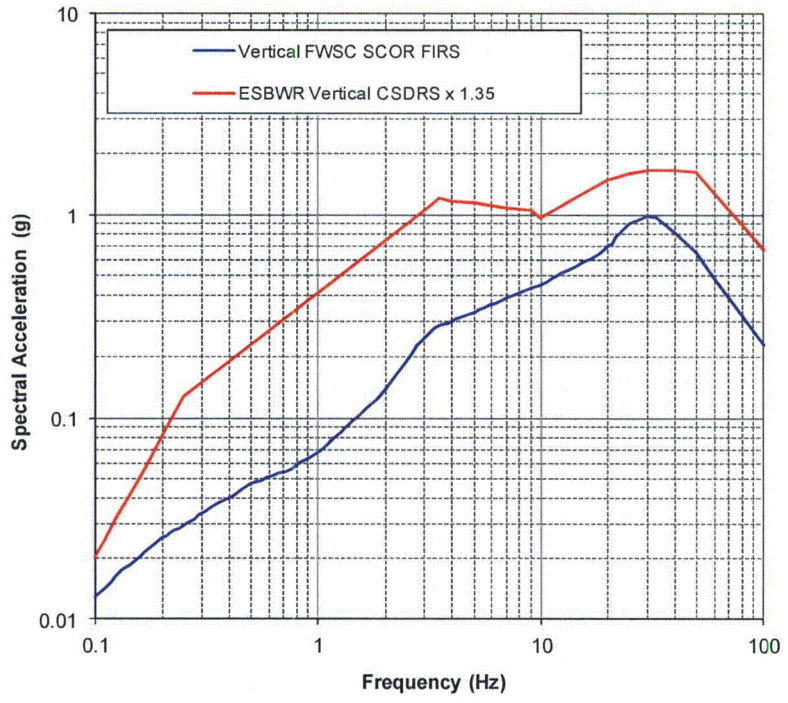

Figure 2.0-204 **Comparison of Vertical CSDRS with the Unit 3 FIRS for the FWSC** [EF3 COL 2.0-1-A]

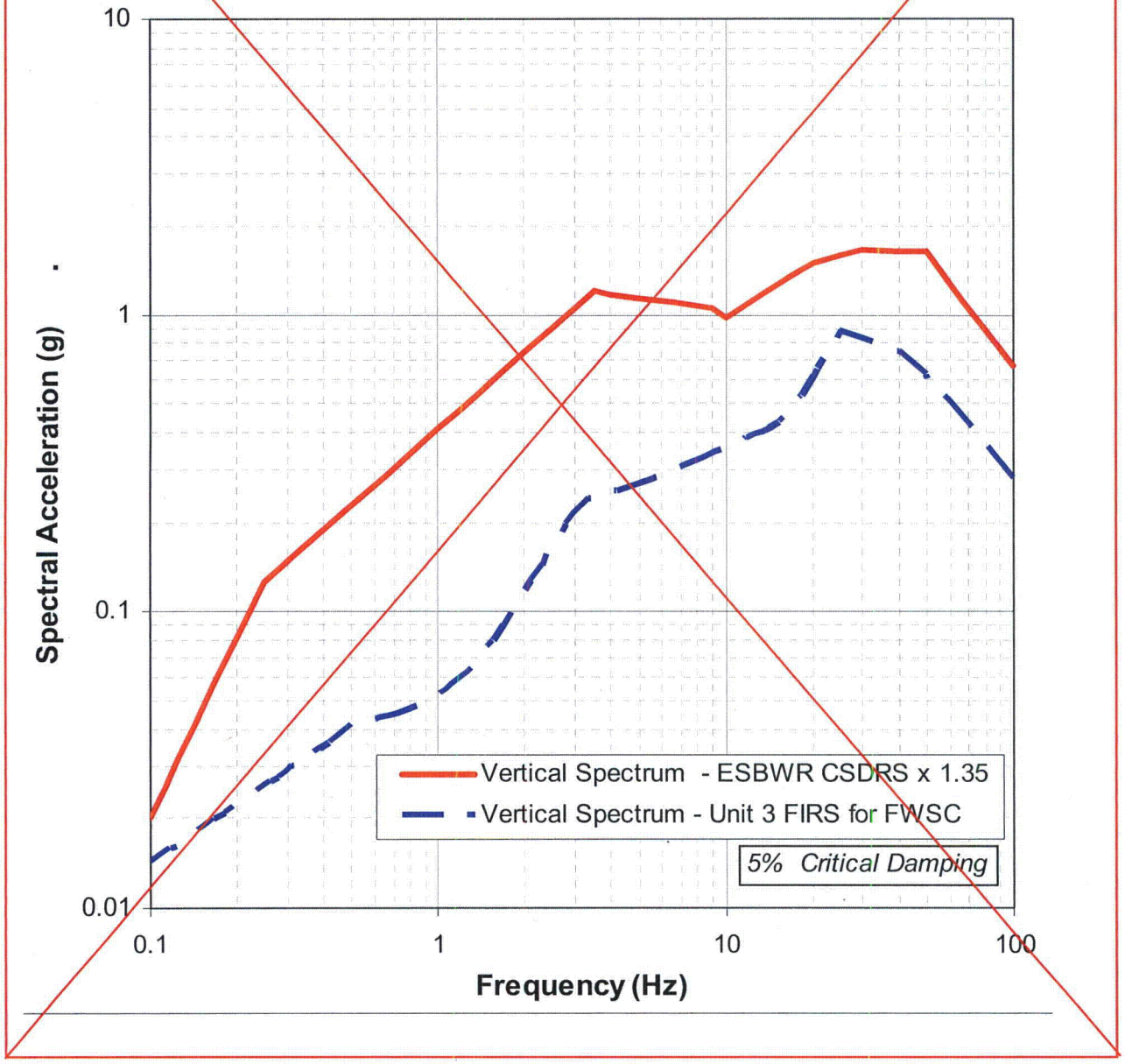

clayey texture evolved with the second regional advance of the late Wisconsinan as ice incorporated lacustrine clay as it readvanced through proglacial lake basins (Reference 2.5.1-247; Reference 2.5.1-248).

2.5.1.1.4 Regional Tectonic Setting

The seismotectonic framework of a region, which includes the basic understanding of existing tectonic features and their relationship to the contemporary stress regime and seismicity, forms the foundation for assessments of seismic sources. ~~In the probabilistic seismic hazard study performed by the Electric Power Research Institute and Seismic Owners Group (EPRI SOG) in 1988 (Reference 2.5.1-286), seismic source models were developed for the Central and Eastern United States (CEUS) based on tectonic setting, the identification and characterization of "feature specific" source zones, and the occurrence, rates, and distribution of historical seismicity. The EPRI models reflected the general state of knowledge of the geosciences community in the mid- to late 1980s.~~

Insert 5

~~Additional geologic, seismologic, and geophysical research has been performed in the site region since the EPRI SOG study (Reference 2.5.1-286). This section presents a summary of the current state of knowledge of the regional tectonic setting and provides more recent information that is relevant to the identification of seismic sources for Fermi 3.~~ The following sections describe the region in terms of (1) the contemporary tectonic stress environment (Subsection 2.5.1.1.4.1); (2) regional geophysical data sets that have been used to evaluate basement geology and structures (Subsection 2.5.1.1.4.2); (3) primary structural provinces and tectonic features within the 320 km (200 mi) radius of the site (Subsection 2.5.1.1.4.3); and (4) significant seismic sources at distances greater than 320 km (200 mi) (Subsection 2.5.1.1.4.4). ~~Historical seismicity is shown on Figure 2.5.1-207 described in Subsection 2.5.1.1.4 and discussed in more detail in Subsection 2.5.2.1.~~

Prehistoric, historical, and instrumental seismicity is shown on Figure 2.5.1-207 and is described in Subsection 2.5.1.1.4.3 and Subsection 2.5.1.1.4.4. The historical and instrumental earthquake catalog for the Fermi 3 site is updated from the CEUS SSC earthquake catalog presented in NUREG-2115 (Reference 2.5.1-286), and is described in Subsection 2.5.2.1.

2.5.1.1.4.1 Contemporary Tectonic Stress Environment

Fermi 3 lies within a compressive midplate stress province, characterized by a relatively uniform east-northeast compressive stress field that extends from the midcontinent east toward the Atlantic continental margin and possibly into the western Atlantic basin (Reference 2.5.1-287). Zoback and Zoback (Reference 2.5.1-287) note

Insert 5

In January 2012, the Electric Power Research Institute/U.S. Department of Energy/U.S. Nuclear Regulatory Commission (EPRI/USDOE/USNRC) published as NUREG-2115 the Central and Eastern United States Seismic Source Characterization (CEUS SSC) model (Reference 2.5.1-286) for use in assessing seismic hazard at nuclear facilities. As discussed in Subsection 2.5.2, the CEUS SSC model is used as the basis for characterizing the seismic hazard at the Fermi 3 site. The CEUS SSC model incorporates the latest knowledge of the geosciences community on seismic hazards in the CEUS. This section presents a summary of the current state of knowledge on the tectonic setting of the Fermi 3 site. The information presented in this section is relevant to characterization of seismic sources that was used in the development of the CEUS SSC model.

define Class A features as those where geologic evidence demonstrates the existence of a Quaternary fault of tectonic origin. Class B features are those where the fault may not extend deeply enough to be a potential source of significant earthquakes, or where the currently available geologic evidence is not definitive enough to assign the feature to Class C or to Class A. Class C features are those for which geologic evidence is insufficient to demonstrate the existence of a tectonic fault, Quaternary slip, or deformation associated with the feature. Crone and Wheeler (Reference 2.5.1-316) identify two Class C seismic zones in the site region that are described below in Subsection 2.5.1.1.4.3.3.

The CEUS SSC study (Reference 2.5.1-286) does not identify any Repeated Large Magnitude Earthquake (RLME) seismic sources within 320 km (200 mi) of the Fermi 3 site.

A description of major basins and arches in the site region is provided in Subsection 2.5.1.1.4.3.1; specific tectonic features and structures are described in Subsection 2.5.1.1.4.3.2; and seismic zones in the site region are described in Subsection 2.5.1.1.4.3.3.

2.5.1.1.4.3.1 Basins and Arches

Intracratonic basins and bounding arches developed in the (200 mi-radius) site region during the Paleozoic (570 – 250 Ma) and include the Michigan, Illinois, and Appalachian basins, and the Cincinnati, Kankakee, Findlay, and Algonquin arches (Figure 2.5.1-208 and Figure 2.5.1-218). The most significant with respect to the site are the Michigan basin and the Findlay and Algonquin arches. In addition to these structures, the now outdated name "Washtenaw Anticlinorium" was proposed by Ells (Reference 2.5.1-318) to describe a broad northwest plunging structure in southeast Michigan and was discussed in the Fermi 2 UFSAR (Reference 2.5.1-221). As defined, local structures included within this broad structural feature are the Bowling Green (Lucas-Monroe) fault/anticline (northern segment) and the Howell (Howell-Northville) anticline/fault described in Subsection 2.5.1.1.4.3.2.

2.5.1.1.4.3.1.1 Michigan Basin

The intracratonic Michigan basin is nearly circular, about 400 km (240 mi) in diameter, and 5 km (3 mi) deep. The basin exhibits only minor syndepositional (contemporaneous with sedimentation) faulting that has an insignificant effect on basin-scale geometry of stratigraphic units (Reference 2.5.1-240). The proto-Michigan basin developed in the Late Cambrian with the deposition of the Mount Simon Sandstone in an elongate trough, possibly representing a northern continuation of the Reelfoot rift – Illinois basin (Reference 2.5.1-240). Basin-centered

The geometry of the Akron-Suffield-Smith Township faults suggest that they originated as en-echelon, synthetic faults produced by right-lateral wrenching, with inferred minimum displacement of 21 km (13 mi) and subsequent normal displacements on the faults (Reference 2.5.1-342). Displacement on the Precambrian unconformity surface is 60 – 120 m (200 – 400 ft), while maximum vertical displacement of the Devonian Onondaga Limestone across the Akron-Suffield faults is 60 m (200 ft) and across the Highlandtown fault it is 72 m (240 ft) (Reference 2.5.1-342). Hook and Ferm (Reference 2.5.1-343) postulate that deposition of the Linton channel deposits below the Middle Pennsylvanian (Westphalian D) Upper Freeport coal may have been controlled by movement on the Transylvania fault extension in Cambrian through Lower Carboniferous strata (Pittsburgh-Washington cross-strike structural discontinuity). Post-Lower Pennsylvanian faulting cannot be assessed because of the absence of younger units. The northeast-southwest-trending Akron magnetic boundary crosses between the Middleburg and Akron faults.

The Transylvania fault extension is overlain by alluvium and colluvium of Middle Pleistocene to Holocene age (Reference 2.5.1-207). There is no known evidence of Quaternary tectonic faulting in Ohio.

2.5.1.1.4.3.3 Seismic Zones

Earthquakes in the site region are generally shallow events associated with reactivated Precambrian faults favorably oriented in the modern northeast-southwest compressive stress regime (Reference 2.5.1-344). None of these events has associated surface rupture, and no faults in the site region exhibit evidence of movement since the Paleozoic (Reference 2.5.1-344). Two seismic zones in the study region, the Anna seismic zone and the northeast Ohio seismic (Figure 2.5.1-207) are designated as Class C features in the USGS Quaternary fault and fold database (Reference 2.5.1-316).

2.5.1.1.4.3.3.1 Northeast Ohio Seismic Zone

The Northeast Ohio seismic zone, also called the Ohio-Pennsylvania seismic zone, defines an approximately 50 km (30.5 mi) long, northeast-southwest-trending zone of earthquakes south of Lake Erie on the Ohio-Pennsylvania border (Figure 2.5.1-207) (Reference 2.5.1-328). The largest historic event in this zone was the January 31, 1986, magnitude (m_b) 5.0 event located about 40 km (24.4 mi) east of Cleveland in southern Lake County, Ohio, and about 17 km (10.4 mi)

Footnote 1: Magnitudes are reported in the magnitude scale designated in the cited reference. E[**M**] is expected moment magnitude and is the uniform magnitude scale used in the project earthquake catalog as described in Subsection 2.5.2.1.

(E[**M**][1] 4.65)

(m_{bLg}) 3.8 (E[**M**] 3.61) earthquake on July 13, 1987; a m_{bLg} 4.3 (E[**M**] 3.86) earthquake on January 26, 2001, which had a MMI of VI; followed by a m_{bLg} 3.0 (E[**M**] 2.92) earthquake on June 3, 2001; and a m_{bLg} 2.3 earthquake on June 5, 2001 (Reference 2.5.1-347). The June 5, 2001, earthquake is not included in the CEUS SSC earthquake catalog of NUREG-2115 due to its small size (E[**M**] less than 2). An event on January 20, 2001, is identified as a blast in the CEUS SSC earthquake catalog. The latest subsequence started in July 2003 with a m_{bLg} 2.5 (E[**M**] 2.29) earthquake (Reference 2.5.1-455).

In 1987, the first in a series of earthquakes continuing to 2003 occurred within the Northeast Ohio seismic zone near Ashtabula in Ashtabula County, Ohio, northeast of the 1986 earthquakes (Reference 2.5.1-347, Reference 2.5.1-455). The largest events in the sequence include an initial Lg wave magnitude ~~(M_{bLg}) 3.8 event on July 13, 1987; a M_{bLg} 2.6 foreshock event on January 19, 2001; a M_{bLg} 4.3 event on January 26, 2001, which had a MMI of VI, followed by a M_{bLg} 3.0 event on June 3, 2001; and a M_{bLg} 2.4 event on June 5, 2001 (Reference 2.5.1-347). The latest subsequence started in July 2003 with a M_{bLg} 2.5 event (Reference 2.5.1-455).~~

Seeber et al. (Reference 2.5.1-455) discuss these fore-main-aftershock sequences and interpretations of these events based on information obtained from three short-term deployments of portable seismographs (in 1987, 2001, 2003) and from regional broadband seismograms. The main observations and conclusions from this analysis are as follows:

- A persistent earthquake sequence in northeast Ohio includes multiple distinct fore-main-aftershock sequences that illuminate two faults approximately 4 km (2.5 mi) apart (Figure 2.5.1-267).
- The seismicity is closely associated with injection of waste fluid in the basal Paleozoic formation from 1986 to 1994.
- All the earthquakes originated from a relatively small area (~ 10 km [6 mi] wide) and are assumed to form a single sequence of casually related earthquakes.
- Felt earthquakes started in 1987, a year after the onset of injection. At that time earthquakes were located 0.7 – 2.0 km (0.4 - 1.2 mi) from the injection site. Seismicity continued and in 2001, 5.5 years after the end of injection, hypocenters were then 5 – 9 km (3 - 6 mi) from the injection site. The only known episode of seismicity in Ashtabula is closely associated with the 1986 – 1994 Class 1 injection, and the pattern of accurate hypocenters is consistent with the one expected for the high pore-pressure anomaly spreading from the injection site.
- This correlation is strong evidence that the seismicity was triggered by the injection.

The July 13, 1987, main shock was close to a deep Class I injection well that was pumping fluids into the Mount Simon Sandstone, the basal Paleozoic unit overlying Precambrian crystalline basement, at a depth of about 1.8 km (1.1 mi), and a number of portable seismographs were

deployed to study the aftershocks (Reference 2.5.1-347). The first 13 well-recorded aftershocks defined a nearly vertical fault with a north-northeast orientation (Reference 2.5.1-245). Analysis of a larger set of well-located aftershocks (36) indicates a cluster in a narrow (0.25 km [0.15 mi] wide), east-striking vertical zone about 1.5 km (1 mi) long, extending from a depth of 1.7 km (1 mi) to 3.5 km (2.1 mi) (Reference 2.5.1-346, Figure 2.5.1-266). The first motions are consistent with left-lateral strike-slip movement on an east-west-striking fault, referred to as the Ashtabula fault (Reference 2.5.1-346). The temporal and spatial proximity between injection and earthquake generation suggested that the injection of waste fluids, which commenced in 1986, triggered the seismicity (Reference 2.5.1-345; Reference 2.5.1-346). Seeber and Armbruster concluded that the zone of seismicity represented a pre-existing basement fault brought to failure by the fluid flow and/or increased pore pressure induced by fluid injection. Seeber and Armbruster noted that from 1987 to 1992, the seismicity appeared to migrate westward out to a distance of 5 to 10 km (3 - 6 mi), possibly along the Ashtabula fault. However, in a more recent paper, Seeber et al. (Reference 2.5.1-455) revised their interpretation to conclude that the linear patch of 1987 earthquakes is a portion of the fault activated by high pore pressure rather than a single rupture. Due to poor location constraints on earthquakes from August 1987 to 2001, the location of the M 2.9 earthquake on March, 28, 1992, cannot be definitely associated with the Ashtabula fault (Reference 2.5.1-455).

(E[**M**] 2.63)

The Ohio Seismic Network was installed in 1999 and precisely recorded the 2001 earthquakes (Reference 2.5.1-347). ~~After a felt M_{bLg} 2.6 foreshock on January 20, 2001, an M_{bLg} 4.3 main shock caused slight damage (MMI VI) on January 26.~~ A focal mechanism obtained by modeling regional waveforms of ~~this~~ earthquake is consistent with composite focal mechanisms from locally recorded earthquakes. Well-located aftershocks of the June 3, 2001, ~~M_{bLg}~~ 3.0 and July 17, 2003, ~~M_{bLg}~~ 2.5 earthquakes define a 5 – 7 km (3 - 4 mi) long plane striking 96 degrees and dipping 65 degrees south. (Reference 2.5.1-455, Figure 2.5.1-266) Seeber et al. (Reference 2.5.1-455) interpret this plane as the source fault for the 2001 seismicity, which resembles the postulated 1.5 km (0.9 mi) long, east-west-striking basement fault having left-lateral slip defined by the 1987 seismicity.

the m_{bLg} 4.3 (E[**M**] 3.86)

(E[**M**] 2.92)

(E[**M**] 2.29)

m_{bLg}

m_{bLg}

Additional documentation of the 1995 paleoliquefaction field search in northeastern Ohio, which focused on the vicinity of the nuclear power plant near Perry, Ohio, was provided to the U.S. Nuclear Regulatory Commission (NRC) in a letter report submitted by Dr. Obermeier to Dr. Andrew Murphy on May 23, 1996 (Reference 2.5.1-483). From the ages and liquefaction susceptibility of the sediments observed during the reconnaissance, Dr. Obermeier made the following conclusions specific to the Perry nuclear plant:

> "...within 20 km of the plant, the lack of suitable exposures precludes definitive statements concerning whether or not there has been strong seismic shaking for most of Holocene time."
>
> "The lack of exposures with liquefiable sediment more than a few thousand years old, within 20 to 25 km of the plant, precludes any statement concerning whether there could have been strong shaking at the plant locale from even moderate-sized earthquakes (say, M ~ 6) occurring more than a few thousand years ago."
>
> "...one large sand and gravel pit (Pit-CL) of latest Pleistocene sediment, probably with a moderate to high liquefaction susceptibility, is located within 32 km of the plant...The lack of liquefaction features indicates a lack of strong seismic shaking through most or all Holocene time."

The CEUS SSC model presented in NUREG-2115 (Reference 2.5.1-286) utilizes broad regional seismic source zones to represent the occurrence of distributed seismicity in the CEUS. Earthquake recurrence rates are modeled as spacially variable in cells with dimensions of ¼ degree longitude by ¼ degree latitude or ½ degree longitude by ½ degree latitude. As such, the Northeast Ohio seismic zone appears as an area of higher seismicity rate within the larger regional source zones in which it lies (Subsection 2.5.2.2.1).

~~The Northeast Ohio seismic zone was included in alternative smaller seismic source zones by two of the EPRI SOG Earth Science Teams (EST), the Rondout and Woodward Clyde Consultants teams, and was partly incorporated into a smaller zone by a third team (Bechtel team) (see Subsection 2.5.2).~~

2.5.1.1.4.3.3.2 **Anna Seismic Zone**

The Anna seismic zone, also called the Western Ohio seismic zone, coincides with northwest-southeast-trending basement faults associated with the Fort Wayne rift in Shelby, Auglaize, and nearby counties (Figure 2.5.1-207) (Reference 2.5.1-344). Ruff et al. (Reference 2.5.1-348) attribute seismicity to the Anna-Champaign, Logan, and Auglaize faults. This zone has produced at least 40 felt earthquakes since 1875, including events in 1875, 1930, 1931, 1937, 1977, and 1986 that caused minor to moderate damage (Reference 2.5.1-344). The July 12, 1986, event near the town of St. Marys in Auglaize County was the largest earthquake to occur in the zone since 1937 (Reference 2.5.1-344). Schwartz and Christensen (Reference 2.5.1-349) determined a hypocenter of 5 km (3 mi) for the magnitude (m_b) 4.5 ~~event~~ and a focal mechanism (strike = 25°, dip = 90°, rake = 175°) representing mostly

(E[**M**] 4.37) earthquake

strike-slip with a small oblique component approximately parallel to the Anna-Champaign fault and a nearly horizontal *P* axis oriented east-northeast. The earthquake produced an MMI V1 event (Reference 2.5.1-349). Hansen (Reference 2.5.1-344) concluded that the historic record indicates a maximum magnitude of 5, but suggested that this zone was capable of producing a magnitude 6.0 to 7.0 event. Obermeier (Reference 2.5.1-350) investigated stream banks in the vicinity of Anna, Ohio, and portions of the Auglaize, Great Miami, Stillwater, and St. Marys rivers and found no evidence of paleoliquifaction features indicative of a magnitude 7 event in the past several thousand years. Crone and Wheeler (Reference 2.5.1-316) designated the Anna seismic zone as a Class C feature based on the occurrence of significant historical earthquakes and the lack of paleoseismic evidence. ~~With the exception of one team (Law Engineering), the EPRI SOG ESTs included smaller source zones to account for the concentration of seismicity in the Anna seismic zone (Subsection 2.5.2).~~

The Anna seismic zone is represented in the CEUS SSC model as an area of higher seismicity rate within the larger regional source zones in which it lies (Subsection 2.5.2.2.1).

2.5.1.1.4.4 Significant Seismic Sources at Distance Greater than 320 Km (200 Mi)

More distant sources of large-magnitude earthquakes are the New Madrid seismic zone (NMSZ) and the Wabash Valley seismic zone (WVSZ), which are approximately 800 km (500 mi) and 500 km (300 mi) southwest, respectively, from Fermi 3 (Figure 2.5.1-207). ~~The results of the 1989 EPRI study (Reference 2.5.1-351) indicated that neither the NMSZ nor the WVSZ sources contributed to 99 percent of the hazard at Fermi 2. New information developed since the EPRI SOG study, however, indicates changes in the frequency or magnitude of large magnitude events that are expected to occur within these seismic zones, and this information is considered in updating the EPRI hazard model for this study (Subsection 2.5.2). Recent evaluations and new information used to update the source characterizations are described below.~~

The CEUS SSC study (NUREG-2115) characterizes RLME seismic sources in the NMSZ and the WVSZ. As described in Subsection 2.5.2.4.4, these RLME seismic sources contribute to the seismic hazard at the Fermi 3 site. Recent information used in NUREG-2115 to characterize these sources is described below.

2.5.1.1.4.4.1 New Madrid Seismic Zone

The New Madrid seismic zone (NMSZ) lies within the Reelfoot rift and is defined by post-Eocene to Quaternary faulting, and historical seismicity (Reference 2.5.1-316). The NMSZ, which is approximately 200 km (124 mi) long and 40 km (25 mi) wide, extends from southeastern Missouri to northeastern Arkansas and northwestern Tennessee (Figure 2.5.1-207).

A number of models have been proposed to explain the origin of stresses driving active deformation in the CEUS. Several of the models provide explanations for localization of seismicity and recurrence of large-magnitude events in the NMSZ, as follows:

- The presence of a rift pillow (body of igneous rock in the crust composed of injected high-density mantle material) underlying the Reelfoot rift (Reference 2.5.1-456) causes local stress concentration (Reference 2.5.1-457).
- A weak subhorizontal detachment fault exists in the lower crust above the rift pillow that causes local stress concentration (Reference 2.5.1-458).
- High local heat flow creates high ductile strain rates in the upper mantle and lower crust, causing seismicity in the upper crust (Reference 2.5.1-459; Reference 2.5.1-476).
- Glacial unloading north of the NMSZ at the close of the Wisconsinan increased seismic strain rates in the NMSZ and initiated the Holocene seismicity (Reference 2.5.1-460).
- Some local or regional perturbation of the stress field, pore pressure, or thermal state is responsible for triggering viscous relaxation of a weak lower-crustal zone within an elastic lithosphere. This may cause a sequence of fault ruptures with short recurrence intervals. A strong candidate for this perturbation is recession of the Laurentian ice sheet, approximately 14 ka. (Reference 2.5.1-461).
- Low-permeability seals form around the fault zone as stress accumulates, raising the pore pressure until an earthquake occurs. Temporal clustering may reflect the evolution of pore fluid pressure in a fault zone. (Reference 2.5.1-462)
- Accelerated Late Wisconsin and Holocene denudation above the NMSZ due to the confluence of the Mississippi and Ohio rivers stepping north to Thebes Gap, perhaps in combination with the retreating Laurentide forebulge, may have been sufficient to initiate Holocene seismicity by causing a perturbation in the local stress field (Reference 2.5.1-461; Reference 2.5.1-463).
- Deep-mantle flow combined with the seismic anisotrophy beneath continents invoke mechanical coupling and subsequent shear between the lithosphere and asthenosphere. Two orthogonal sets of shear zones and faults observed on a continental scale mimic

Modeling studies (Reference 2.5.1-460) show that the removal of the Laurentide ice sheet approximately 20,000 years ago changed the stress field in the vicinity of New Madrid, causing seismic strain rates to increase by about three orders of magnitude. The modeling predicts that the high rate of seismic energy release observed during late Holocene time is likely to continue for the next few thousand years (Reference 2.5.1-460).

magnitude 6.7 to 8.1

(Reference 2.5.1-286)

The NMSZ produced three large-magnitude earthquakes (estimates range from ~~M_w 7.1 to 8.4~~) between December 1811 and February 1812. The actual size of these pre-instrumental events is not known with certainty and is based primarily on various estimates of damage intensity and amount and pattern of liquefaction. (Reference 2.5.1-358; Reference 2.5.1-359; Reference 2.5.1-360; Reference 2.5.1-361)

; Reference 2.5.1-366; Reference 2.5.1-499; Reference 2.5.1-500

The December 16, 1811, earthquake is inferred to be associated with strike-slip displacement along the southern portion of the NMSZ (Reference 2.5.1-361; Reference 2.5.1-356). Johnston (Reference 2.5.1-361) estimated the December event to have a magnitude of ~~M_w~~ 8.1 ± 0.31. Hough et al. (Reference 2.5.1-360) later re-evaluated the intensity data for the region and concluded that the event had a magnitude of M_w 7.2 to 7.3. Bakun and Hopper (Reference 2.5.1-358) also re-evaluated the intensity data and derived a preferred magnitude of ~~M_w~~ 7.6 for the December 1811 event.

M

M

More recently, Hough and Page (Reference 2.5.1-500) assessed the magnitude to be M_w 6.7 to 6.9.

The February 7, 1812, New Madrid earthquake is associated with reverse displacement along the middle part of the NMSZ (Figure 2.5.1-207) (Reference 2.5.1-362; Reference 2.5.1-363; Reference 2.5.1-356; Reference 2.5.1-358; Reference 2.5.1-361). This earthquake most likely occurred along the northwest-trending Reelfoot fault that extends approximately 69 km (43 mi) from northwestern Tennessee to southeastern Missouri (Reference 2.5.1-364; Reference 2.5.1-365). The Reelfoot fault is a northwest-trending southwest-vergent (shortening direction) reverse fault (Reference 2.5.1-363; Reference 2.5.1-366). It forms a topographic scarp developed as a result of fault-propagation folding (Reference 2.5.1-363; Reference 2.5.1-365). Kelson et al. (Reference 2.5.1-363) investigated near-surface deformation along the trace of the scarp and found evidence for three events within the past 2, 400 years. The most recent event was associated with the 1811/1812 earthquake sequence. The penultimate event is estimated to have occurred between A.D. 1260 and 1650. The pre-penultimate event occurred prior to about A.D. 780 to 1000. A range of recurrence intervals for the Reelfoot fault are estimated between 150 to 900 years, with a preferred range of about 400 to 500 years (Reference 2.5.1-363). The geometry and reverse sense of motion of the Reelfoot fault implies that this structure serves as a step-over segment between the southern and northern portions of the fault system (Reference 2.5.1-352;

Reference 2.5.1-316). Johnston (Reference 2.5.1-361) estimated a magnitude of ~~M_w~~ 8.0 ±_0.33 for the February 1812 event. Hough et al. (Reference 2.5.1-360) later re-evaluated the intensity data for the region and concluded that the February event had a magnitude of M_w 7.4 to 7.5. Bakun and Hopper (Reference 2.5.1-358) also re-evaluated the intensity data from the 1811/1812 sequence and derived a preferred magnitude of ~~M_w~~ 7.8 for the event.

Hough and Page (Reference 2.5.1-500) assess the magnitude to be M_w 7.1 to 7.3.

The January 23, 1812, earthquake is inferred to be associated with strike-slip displacement on the New Madrid North fault along the northern portion of the NMSZ (Figure 2.5.1-207) (Reference 2.5.1-356). The interpretation that the January 1812 earthquake occurred along the New Madrid North fault of the NMSZ is based on fault mechanics and limited historical data, and is more poorly constrained than interpretations of the December 16, 1811, and February 7, 1812, earthquakes. Baldwin et al. (Reference 2.5.1-367) conducted paleoseismic investigations along this segment of the fault and although their investigations identified liquefaction evidence for the 1811/1812 earthquake sequence, their data does not support the presence of a major through going fault with repeated late Holocene events.

Johnston (Reference 2.5.1-361) estimated a magnitude of ~~M_w~~ 7.8 ± 0.33 for the January 1812 event. Hough et al. (Reference 2.5.1-360) later re-evaluated the intensity data for the region and concluded that the January event had a magnitude of ~~M_w~~ ~~7.1~~ M_w 7.0. Bakun and Hopper (Reference 2.5.1-358) also re-evaluated the intensity data from 1811/1812 sequence and derived a preferred magnitude of ~~M_w~~ 7.5 for the January 23, 1812, event.

Hough and Page (Reference 2.5.1-500) assess the magnitude to be M_w 6.8 to 7.0.

Because there is little surface expression of faults within the NMSZ, earthquake recurrence estimates are based largely on dates of paleoliquefaction and offset geological features. Tuttle et al. (Reference 2.5.1-368; Reference 2.5.1-369) provide recent summaries of paleoseismologic data that suggest that that the average recurrence interval for surface deforming earthquakes in the NMSZ is about 200 to 800 years, with a preferred estimate of 500 years. ~~The 200- to 800-year recurrence estimate, with a preferred estimate of 500 years is significantly shorter than the 5000 year earthquake recurrence interval used in the 1988 EPRI SOG study based on extrapolation of historical seismicity (see discussion in Subsection 2.5.2).~~ Paleoliquefaction studies document evidence that prehistoric sand blows, such as those formed

Based on considerations of the above information and review of an updated paleoliquefaction database, the CEUS SSC project developed an RLME source to represent the central faults in the NMSZ. This seismic source is modeled as producing recurring earthquakes in the magnitude range of moment magnitude (**M**) 6.7 to 7.9 with average recurrence intervals of approximately 500 years (Reference 2.5.1-286).

during the 1811/1812 earthquakes, probably are compound structures resulting from multiple earthquakes closely clustered in time (earthquake sequences) (Reference 2.5.1-368).

~~The upper bound maximum magnitude values (Mmax) used by the EPRI SOG teams range from mb 7.2 to 7.9 (Subsection 2.5.2). More recent estimates of Mmax as outlined above have generally been within this range. The most significant updates of source parameters for the NMSZ since the 1986 EPRI SOG study (Reference 2.5.1-305) are the reduction in the mean recurrence interval to approximately 500 years and consideration of clustered event sequences.~~

2.5.1.1.4.4.2 Wabash Valley Seismic Zone

M 4 to 5.5 (E[**M**] 4.29 to E[**M**] 5.32)) (Reference 2.5.1-374)

The Wabash Valley region in southeastern Illinois and southwestern Indiana has been an area of persistent seismicity and the site of several moderate-magnitude historical earthquakes (~~estimated moment magnitude (**M**) 4.5 to **M** 5.8; including the April 28, 2008 **M** 5.2 event outside Mt. Carmel, Illinois) (Reference 2.5.1-370)~~ (Figure 2.5.1-207). ~~This region was recognized as a more seismically active region by the EPRI ESTs and was included in source zones that differentiated the region from the adjacent more seismically quiescent craton regions (Subsection 2.5.2).~~ Investigations ~~that post dated the EPRI SOG study~~ have documented evidence for multiple paleoearthquakes having magnitudes significantly larger than historical events that have occurred in the region. Mapping and dating of liquefaction features throughout most of the southern Illinois basin and in parts of Indiana, Illinois, and Missouri identified energy centers for at least eight Holocene and latest Pleistocene earthquakes having estimated moment magnitudes of **M** 6 to **M** 7.8 (~~Figure 2.5.1-207~~) (Reference 2.5.1-371; Reference 2.5.1-372). The WVSZ is designated a Class A feature in the USGS Quaternary fault and fold database of the United States (Reference 2.5.1-370).

Use of a more recently developed magnitude-bound curve for the CEUS based on a value of **M** approximately 7.6 to 7.7 for the largest of the 1811-1812 New Madrid earthquakes (reduced from the higher **M** 8 used by Obermeier [Reference 2.5.1-374] in an earlier curve) gives lower estimates of **M** (Reference 2.5.1-503) as shown on Figure 2.5.1-207.

7.3 to

Liquefaction features from the strongest paleoearthquake, an estimated **M** 7.5 event that occurred in about 6100 years BP in the Wabash Valley, cover an area that has a diameter of about 300 km (180 mi). Based on the size and distribution of the liquefaction features, the location for this earthquake was in the vicinity of Vincennes, Indiana (Reference 2.5.1-370; Reference 2.5.1-373). ~~The data suggest the existence of a source of repeated large magnitude (**M** 7.0 to **M** 7.8) earthquakes in this region (Reference 2.5.1-374).~~ It has been postulated

The proximity of the energy centers for the two largest earthquakes inferred from the paleoliquefaction data (referred to as the Vincennes and Skelton paleoearthquakes) suggests there is a RLME source in the Wabash Valley (Reference 2.5.1-286).

(Reference 2.5.1-373 and Reference 2.5.1-503)

that a broad flexure (bend or stepover) in bedrock structure results in a concentration of stress in this region (Reference 2.5.1-375). This bend or stepover lies near the northern terminus of a 600 km (370 mi) long magnetic and gravity lineament, referred to as the Commerce Geophysical Lineament (CGL), which extends from Vincennes, Indiana, far into Arkansas (Figure 2.5.1-207) (Reference 2.5.1-376; Reference 2.5.1-377). Late Quaternary faulting recently has been identified near this lineament, close to the Missouri-Illinois border (Reference 2.5.1-378). Wheeler and Cramer (Reference 2.5.1-379) discuss the concept of a left-stepover functioning as a restraining bend if the CGL is acting as a right-lateral strike-slip fault in the current tectonic environment. McBride and Kolata (Reference 2.5.1-380) note a possible relationship between the most deformed region of the Precambrian basement (yet to be identified beneath the Illinois basin and the Enterprise subsequence) and some of the largest twentieth-century earthquakes in the central midcontinent. Evaluation of recently acquired industry seismic-reflection profile data from southern Illinois provides additional insights regarding the causative structures for recent earthquakes. McBride et al. (Reference 2.5.1-381; Reference 2.5.1-382) note that earthquakes may be nucleating along compressional structures in crystalline basement and thus may occur in parts of the basin where there are no obvious surface faults or folds. The results of their study suggest that the seismogenic source just north of the New Madrid seismic zone consists, in part, of thrusts in the basement localized along igneous intrusions that are locally coincident with the CGL (Reference 2.5.1-381; Reference 2.5.1-382).

; Reference 2.5.1-501

(e.g., the 1968 m_b 5.5 (E[**M**] 5.32) earthquake)

Insert 6

Morphometric analysis of the land surface, detailed geologic mapping, and structural analysis of bedrock indicate westward-dipping surfaces in the Wabash Valley region along the western edge of the CGL in the restraining bend region (Reference 2.5.1-383). The sources for other prehistoric earthquakes suggested by the inferred locations of energy centers elsewhere in southern Illinois, Missouri, and Indiana are less certain. Su and McBride (Reference 2.5.1-384) suggest that all paleoliquefaction features in south-central Illinois and southeastern Missouri may have been induced by the paleoearthquakes that occurred near the potential seismogenic structures identified in south-central Illinois by the re-analysis of industry seismic-reflection data (i.e., the Louden anticline, Centralia fault zone, and Du Quoin monocline). Inferred paleoearthquake centers in southwestern Indiana are close to the

Insert 6

McBride et al. (Reference 2.5.1-501) further evaluate major structures within the Illinois basin, including the Wabash Valley fault system and the La Salle anticlinal belt and their possible association with historical earthquakes, including the April 3, 1974, m_b 4.7 (E[**M**] 4.29) earthquake and the June 10, 1987, m_b 5.2 (E[**M**] 4.95) earthquake. Analysis of the June 18, 2002, M_w 4.6 (E[**M**] 4.48) earthquake, which occurred on a steeply dipping fault within the Wabash Valley fault system at a depth of about 18 km (11 mi), may suggest that buried faults associated with a possible Precambrian rift system are being reactivated by the contemporary east/east-northeast-trending regional horizontal compressive stress (Reference 2.5.1-502).

Hoosier thrust belt, Mount Carmel fault and Leesville anticline, which are Paleozoic-age faults (Table 2.5.1-201 and Figure 2.5.1-207).

Based on consideration of the above information, the CEUS SSC project developed an RLME source to represent recurrence of large earthquakes in the Wabash Valley seismic zone with moment magnitudes in the range of **M** 6.75 to 7.5.

Given the uncertainty in identifying specific sources for prehistoric earthquakes in the southern Illinois and southern Indiana regions, Cramer et al. (Reference 2.5.1-385) presented alternative source geometries to account for the sources of large-magnitude earthquakes in the Southern Illinois basin. ~~Alternative zones used by the EPRI SOG teams to capture the uncertainty in seismic sources in the Southern Illinois Basin region encompass these alternatives (Subsection 2.5.2). The current version of the model being used to update the 2008 U.S. National Hazard Maps (Reference 2.5.1-386) does not identify a specific zone, but encompasses the Wabash Valley region in the extended margin zone based on the paleoliquefaction evidence for **M** 7.5 earthquakes.~~

~~The most significant update of source parameters for the WVSZ since the EPRI SOG 1986 (Reference 2.5.1-315) study is the estimate for maximum magnitude. The estimated magnitude for the largest identified paleoearthquakes in the WVSZ (approximately **M** 7.5) is at the upper end of the EPRI SOG EST composite assessment for the Wabash Valley southern Illinois sources (Subsection 2.5.2).~~

2.5.1.1.5 Regional Non-seismic Geologic Hazards

The United States Geological Survey has identified several zones of landslides within the (320 km [200 mi] radius) site region (Figure 2.5.1-227; Reference 2.5.1-387). The Kanawha Section of the Appalachian Plateau Physiographic Province is a region of high susceptibility and moderate to high incidence of landslides associated with the weathering of Pennsylvanian- and Permian-age shales and claystones. The Southern New York Section of the Appalachian Plateau Physiographic Province and Central Lowlands Physiographic Province have small regions along major rivers with high incidence of landslides, including the Cuyahoga River near Cleveland and the Maumee River near Toledo. In the vicinity of the Great Lakes moderate susceptibility for landslides exists associated with lacustrine deposits, and moderate incidence for landslides exists associated with wave erosion at the base of cliffs. (Reference 2.5.1-387)

Karst related problems in the (320 km [200 mi] radius) site region are associated with fissures, tubes and caves that are generally less than

2.5.1-282 Wylie, A.S., J.R. Wood, and W.B. Harrison, III, "Michigan Trenton-Black River Opportunities Identified with Sample Attribute Mapping," Oil & Gas Journal, Vol. 102, pp. 29-35, 2004.

2.5.1-283 Mesolella, K.J., J.D. Robinson, L.M. McCormick, and A. R. Ormiston, "Cyclic Deposition of Silurian Carbonates and Evaporites in Michigan Basin," American Association of Petroleum Geologists Bulletin, Vol. 58, pp. 34-62, 1974.

2.5.1-284 Sparling, D.R., "The Bass Islands Formation in its Type Region," *The Ohio Journal of Science*, Vol. 70, pp. 1-33, 1970.

2.5.1-285 Eyles, N., and N.E. Williams, "The Sedimentary and Biological Record of the Last Interglacial-Glacial Transition at Toronto, Canada," in Clark, P.U., and P.D. Lea, eds., "The Last Interglacial-Glacial Transition in North America," Geological Society of America, Special Paper 270, pp. 119 – 137, 1992.

2.5.1-286 ~~Electric Power Research Institute and Seismic Owners Group (EPRI SOG), "Seismic Hazard Methodology for the Central and Eastern United States," Technical Report NP 4726 A, Electric Power Research Institute, Vols. 1 – 10, 1988.~~

Electric Power Research Institute, U.S. Department of Energy, and U.S. Nuclear Regulatory Commission, "Technical Report: Central and Eastern United States Seismic Source Characterization for Nuclear Facilities," NUREG-2115, U.S. Nuclear Regulatory Commission, Washington, D.C., 2012.

2.5.1-287 Zoback, M.L., and M.D. Zoback, "Tectonic Stress Field of the Continental United States," in L.C. Pakiser and W.D. Mooney, eds., "Geophysical Framework of the Continental United States," Geological Society of America, Memoir 172, pp. 523 – 541, 1989.

2.5.1-288 Richardson, R.M., and L.M. Reding, "North American Plate Dynamics," *Journal of Geophysical Research*, Vol. 96, pp. 12, 201 – 12, 223, 1991.

2.5.1-289 Zoback, M.L., "Stress Field Constraints on Intraplate Seismicity in Eastern North America," *Journal of Geophysical Research*, Vol. 97, No. B8, pp. 11, 761 – 11, 782, 1992.

2.5.1-290 Heidbach, O., M. Tingay, A. Barth, J. Reinecker, D. Kurfess, and B. Müller, "The World Stress Map Database Release 2008," doi:10.1594/GFZ.WSM.Rel2008, 2008, http://www.world-stress-map.org, accessed 20 November 2009.

2.5.1-441 National Geophysical Data Center, National Oceanic and Atmospheric Administration (NOAA), "Great Lakes Bathymetry," Bathymetric Data, http://www.ngdc.noaa.gov/mgg/greatlakes/greatlakes.html, accessed 17 August 2007.

2.5.1-442 Michigan Department of Environmental Quality, "Bedrock Geology Map of Michigan," Geologic Survey Division, 1987.

2.5.1-443 Gray, H.H., C.H. Ault, S.J. Keller, and D. Harper, "Bedrock Geologic Map of Indiana," Indiana Geological Survey, Miscellaneous Map 48, scale 1:500,000, 2002.

2.5.1-444 National Geophysical Data Center, National Oceanic and Atmospheric Administration (NOAA), "2-Minute Gridded Global Relief Data (ETOPO2v2) June, 2006," Bathymetric Data, http://www.ngdc.noaa.gov/mgg/fliers/01mgg04.html, accessed 1 January 2007.

(Not Used)

2.5.1-445 ~~Tennessee Valley Authority, "Application for a Combined License (COL) for Two Westinghouse Advance Passive 1000 (AP1000) Pressurized Water Reactors (PWRs) Designated as Bellefonte Nuclear Station Units 3 & 4," date of application submittal October 30, 2007.~~

2.5.1-446 Indiana Geological Survey, "Structural Features of Indiana (Indiana Geological Survey, Line Shapefile," 2002. http://129.79.145.7/arcims/statewide_mxd/dload_page/geology.html, accessed 2 June 2008.

2.5.1-447 Taylor, K.B., R.B. Herrmann, M.W. Hamburger, G.L. Pavlis, A. Johnston, C. Langer, and C. Lam, "The Southeastern Illinois Earthquake of 10 June 1987," *Seismological Research Letters*, Volume 60, No. 3, pp. 101-110, July – September 1989.

2.5.1-448 Slucher, E.R., E.M. Swinford, G.E. Larson, and D.M. Powers, "Bedrock Geologic Map of Ohio," Ohio Geological Survey, Map BG-1, version 6.0, scale 1:500,000, 2006.

2.5.1-449 Armstrong, D.K., and J.E.P. Dodge, "Paleozoic Geology of Southern Ontario," Ontario Geological Survey, Miscellaneous Release — Data 219, 2007.

2.5.1-494 Holcombe, T.L., Taylor, L.A., Warren, J.S., Vincent, P.A., Reid, D.F., and Herdendorf, C.E., "Lake-floor Geomorphology of Lake Erie," National Environmental Satellite, Data, and Information Service, NATIONAL GEOPHYSICAL DATA CENTER, World Data Center A for Marine Geology and Geophysics Research Publication RP-3, 26 pp plus 8 plates and 9 figures, 2005.

2.5.1-495 National Geophysical Data Center, Great Lakes Data Rescue Project – Lake Erie and Lake Saint Clair Bathymetry, "Lake Erie and Lake Saint Clair Geomorphology," http://www.ngdc.noaa.gov/mgg/greatlakes/lakeerie_cdrom/html/e_gmorph.htm.

2.5.1-496 Hobson, G. D., Herdendorf, C.E., and Lewis, F.M., "High Resolution Reflection Seismic Survey in Western Lake Erie," Proceedings of the 12th Conference on Great Lakes Research," pp. 210-224, 1969.

2.5.1-497 Carter, C. H., Williams, S., Fuller, J.A., and Meisburger, E.P., "Regional Geology of the Southern Lake Erie (Ohio) Bottom: A Seismic Reflection and Vibracore Study," U.S. Corps of Engineers Coastal Research Center, Miscellaneous Report No. 82-15, 1982.

2.5.1-498 Black & Veatch letter to Detroit Edison Company, "Denniston Quarry Investigation Technical Memorandum," Letter No. BVDE2- 2010-0038, February 4, 2010.

Insert 7 →

Insert 7

2.5.1-499 Mueller, K., Hough, S.E., and Bilham, R. "Analyzing the 1811-1812 New Madrid earthquakes with recent instrumentally recorded aftershocks," *Nature*, Vol. 429, pp. 284-288, 2004.

2.5.1-500 Hough,S.E., and Page, M., "Toward a consistent model for strain accrual and release for the New Madrid seismic zone, central United States," *Journal of Geophysical Research*, Vol. 116, B03311, 2011.

2.5.1-501 McBride, J.H., Leetaru, H.E., Bauer, R.A., Tingey, B.E., and Schmidt, S.E.A., "Deep faulting and structural reactivation beneath the southern Illinois basin," *Precambrian Research,* Vol. 157, pp. 289-313, 2007.

2.5.1-502 Kim, W.-Y, "The 18 June 2002 Caborn, Indiana, earthquake: Reactivation of ancient rift in the Wabash Valley seismic zone?" *Bulletin of the Seismological Society of America*, Vol. 93, No. 5, pp. 2201-2211, 2003.

2.5.1-503 Olson, S.M., Green, R.A., and Obermeier, S.F., "Revised magnitude bound relation for the Wabash Valley seismic zone of the central United States," *Seismological Research Letters*, Vol. 76, No. 6, pp. 756-771, 2005.

2.5.1-504 Nelson, W.J., "Structural Features in Illinois," Illinois State Geological Survey, Bulletin 100, 1995

Figure 2.5.1-207 Regional Seismicity and Tectonic Features in the Fermi 3 Site Region (Sheet 1 of 3) [EF3 COL 2.0-26-A]

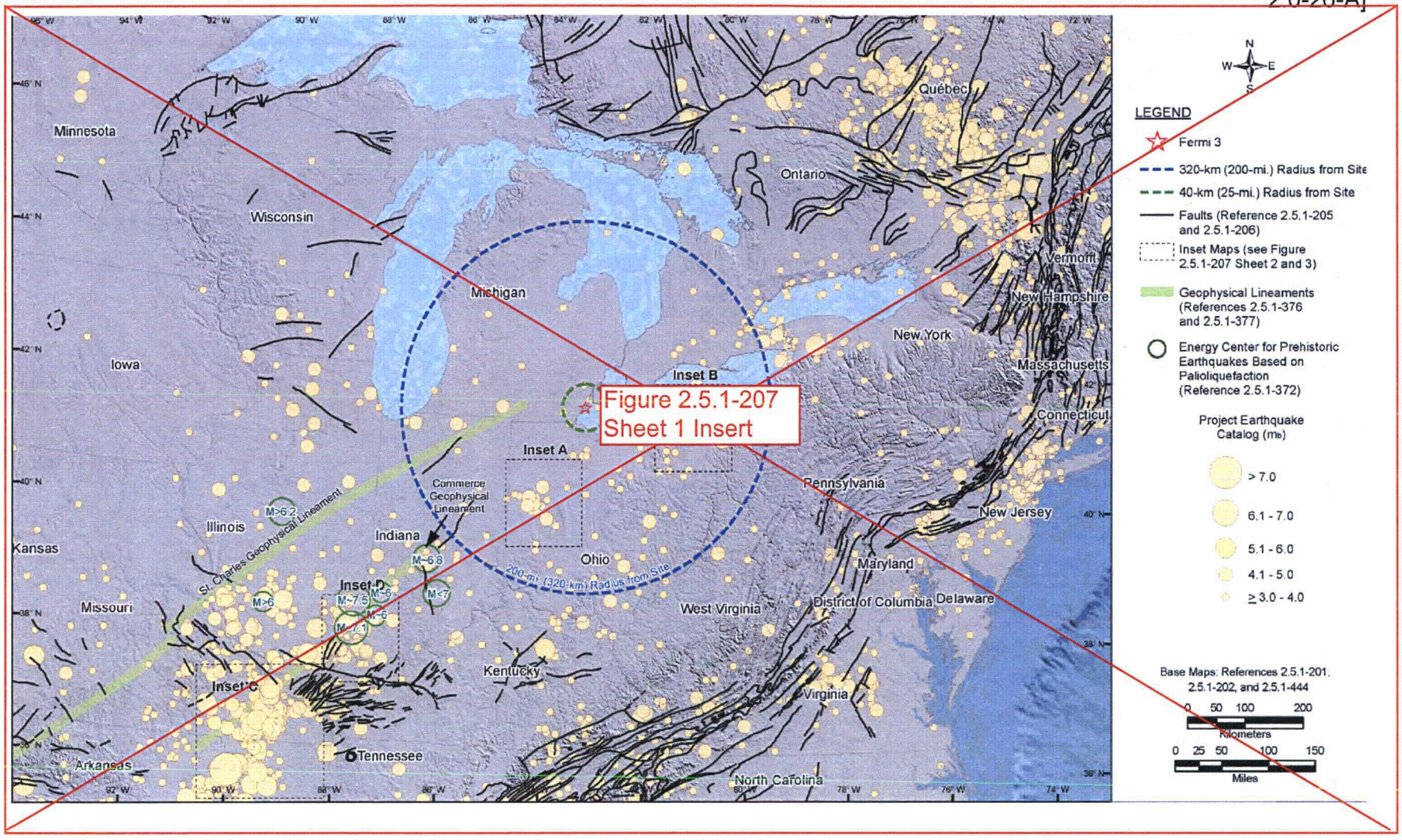

Figure 2.5.1-207 Sheet 1 Insert

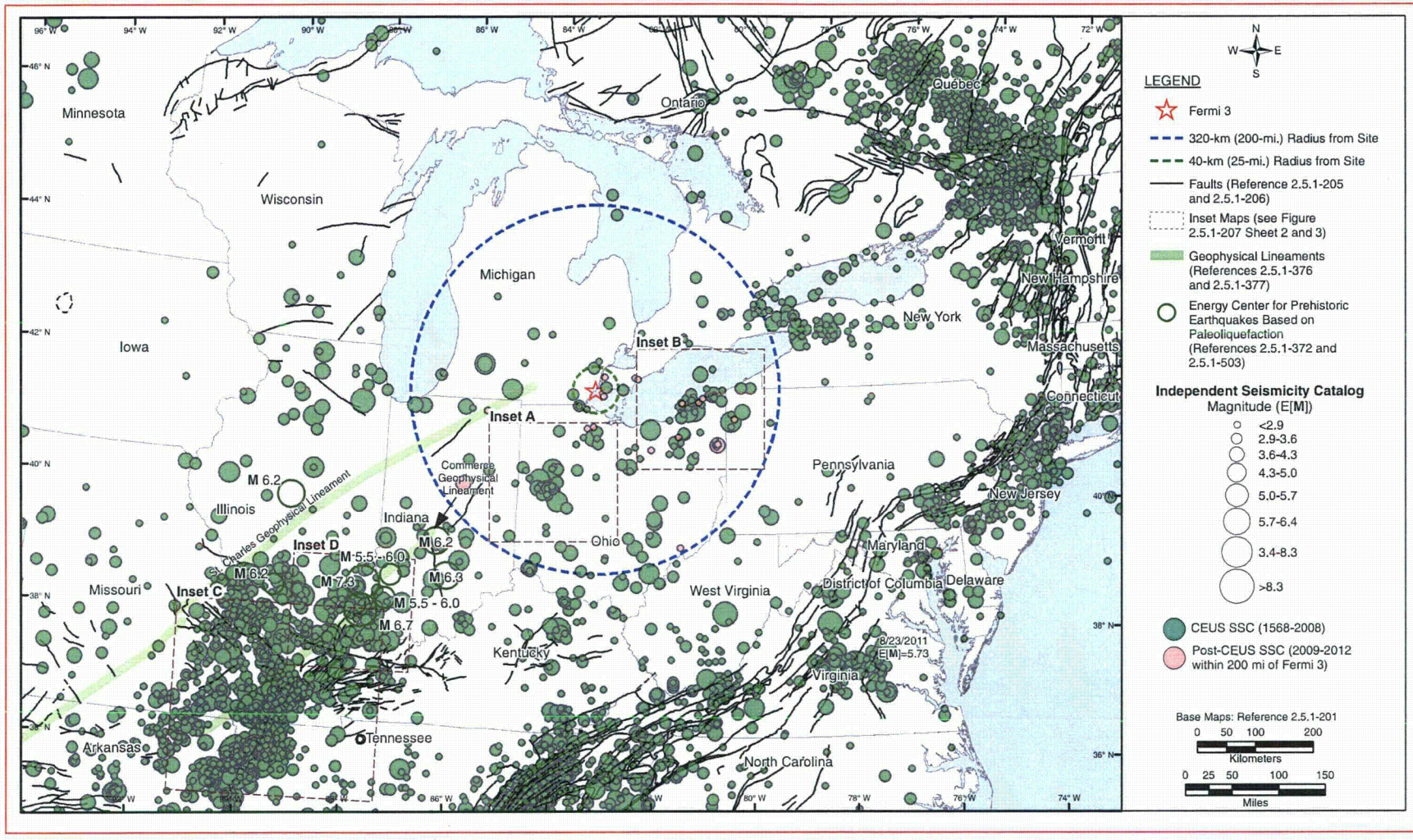

Figure 2.5.1-207 Regional Seismicity and tectonic Features in the Fermi 3 Site Region (Sheet 2 of 3)[EF3 COL 2.0-26-A]

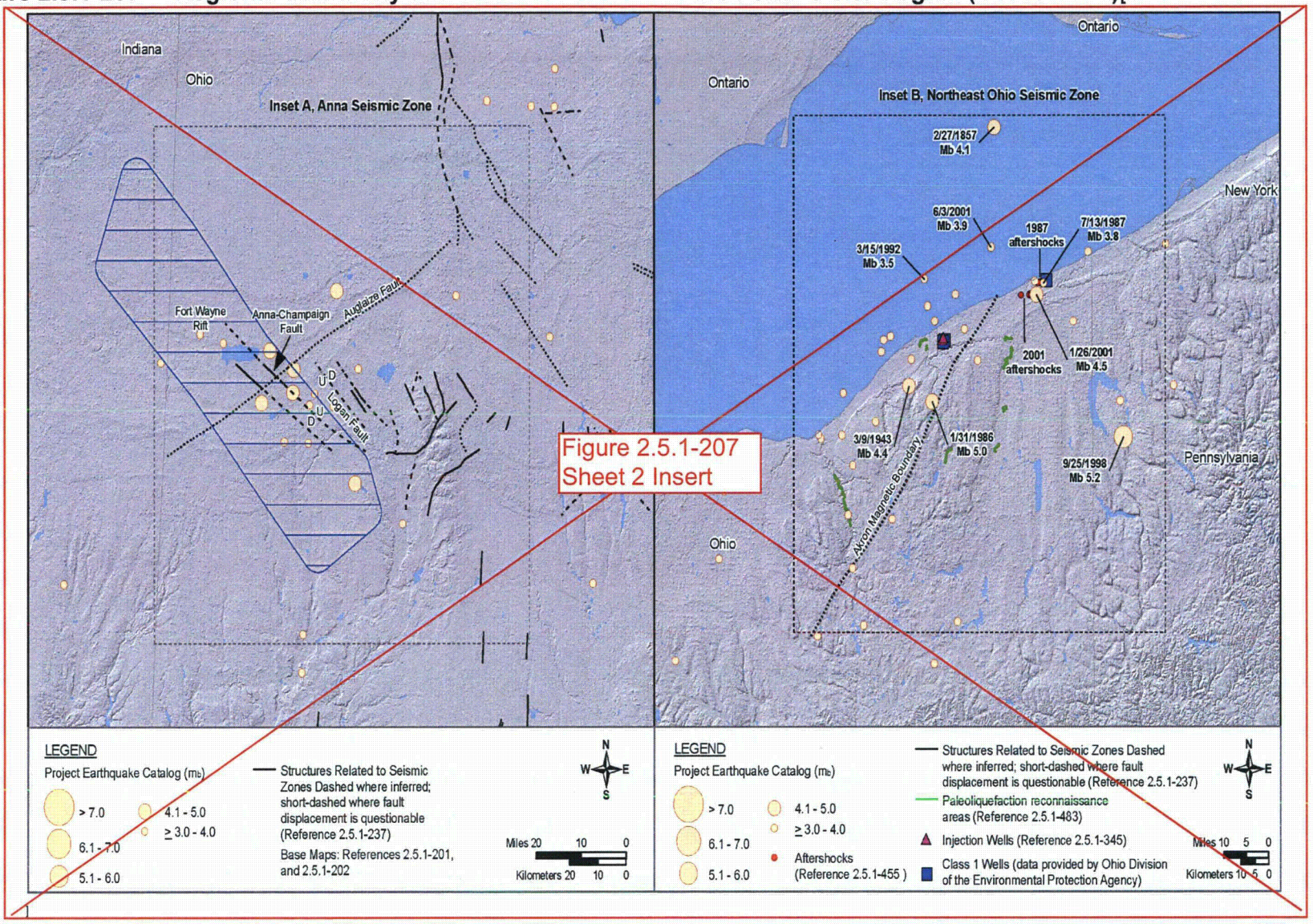

Figure 2.5.1-207 Sheet 2 Insert

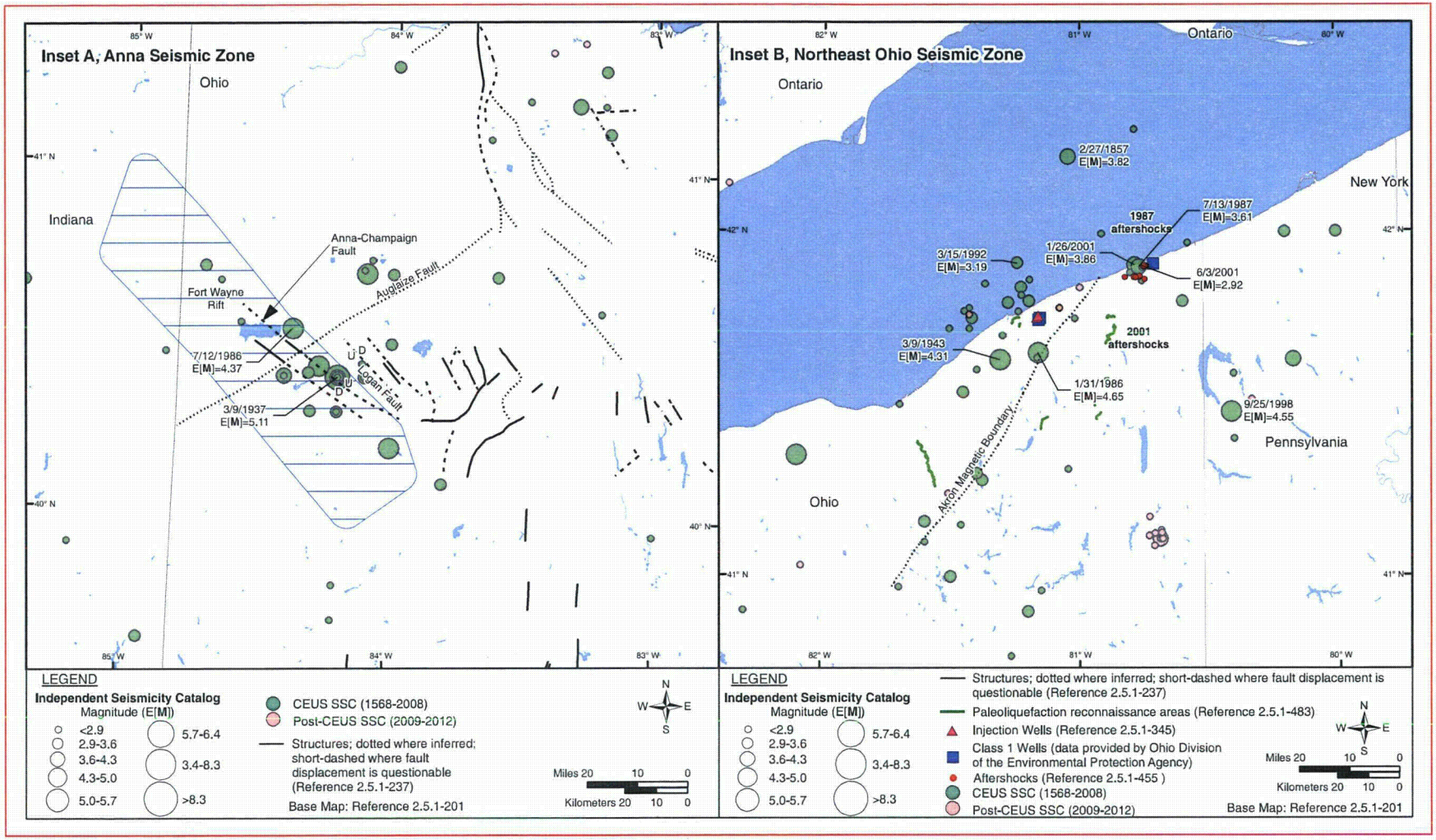

Figure 2.5.1-207 Regional Seismicity and tectonic Features in the Fermi 3 Site Region (Sheet 3 of 3)[EF3 COL 2.0-26-A]

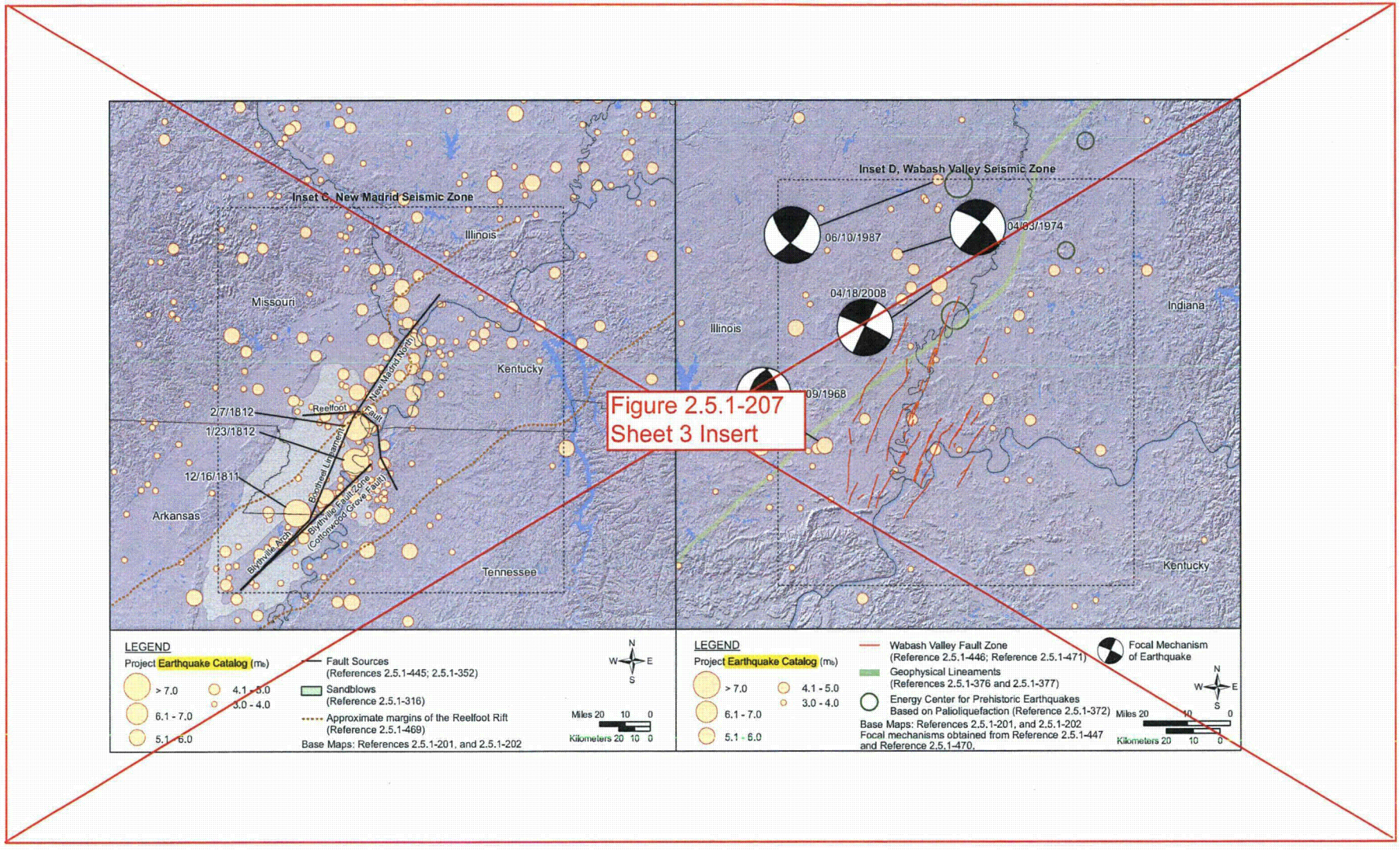

Figure 2.5.1-207 Sheet 3 Insert

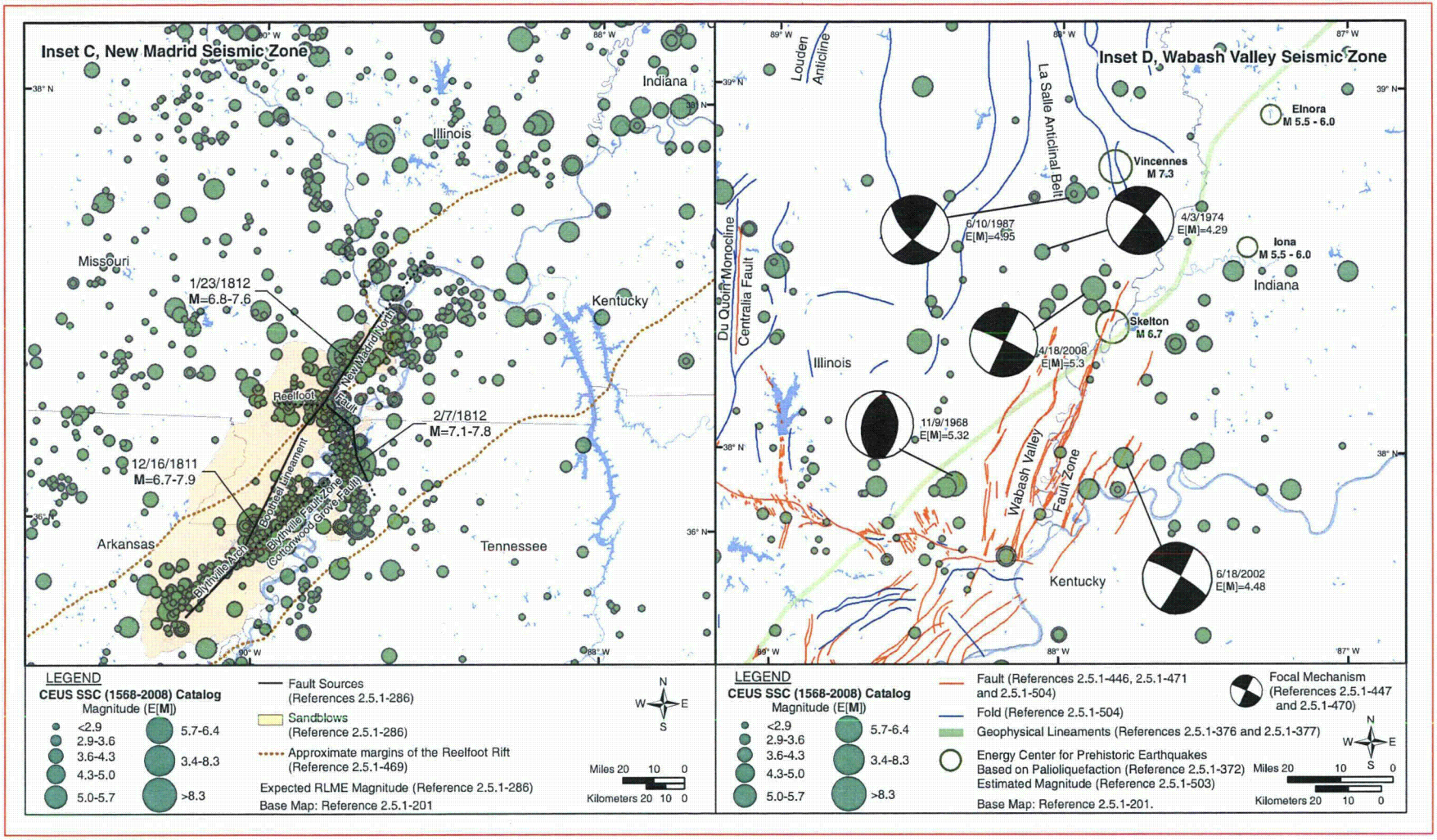

2.5.3-207 Environmental Systems Research Institute (ESRI), ESRI ArcGIS 9.1, Data & Maps, Media Kit, Redlands, California, 2006.

(Not Used)

2.5.3-208 ~~National Aeronautics and Space Administration (NASA)/U.S. Geological Survey (USGS), "SRTM, Shuttle Radar Topography Mission, SRTM 30 data," http://www2.jpl.nasa.gov/srtm/, 2005.~~

2.5.3-209 National Geophysical Data Center, National Oceanic and Atmospheric Administration (NOAA), "Great Lakes Bathymetry," bathymetric data, www.ngdc.noaa.gov/mgg/greatlakes/greatlakes.html, accessed 17 August 2007.

2.5.3-210 Wollensak, M.S., ed., *Oil and Gas Fields of the Michigan Basin*, Volume 1, Michigan Basin Geological Society, 1969.

2.5.3-211 Wollensak, M.S., ed., *Oil and Gas Fields of the Michigan Basin*, Volume 2, Michigan Basin Geological Society, 1991.

2.5.3-212 Tanglis, C. (comp.), "Surface Faults in the Southwestern District, Southern Ontario," Ontario Geological Survey, 1995.

2.5.3-213 Aangstrom Precision Corporation, Structure Contour Maps, Mt. Pleasant, Michigan, 1989.
(a) Dundee Residual Structure Contour Map, scale 1:600,000.
(b) Dundee Structure Contour Map, scale 1:600,000.
(c) Sunbury Shale Residual Structure Contour Map, scale 1:600,000.
(d) Sunbury Shale Structure Contour Map, scale 1:600,000.
(e) Traverse Limestone Residual Structure Contour Map, scale 1:600,000.
(f) Traverse Limestone Structure Contour Map, scale 1:600,000.

2.5.3-214 Baranoski, M.T., "Structure Contour Map on the Precambrian Unconformity Surface in Ohio and Related Basement Features," Ohio Geological Survey Map PG-23, Columbus, Ohio, scale 1:500,000, with 18-page description, available on CD-ROM, 2002.

2.5.3-215 Michigan Department of Natural Resources, "Quaternary Geology of Michigan," Edition 2.0, digital map, 1998.

Figure 2.5.3-201 Map Showing Mapped Structures and Seismicity in the Site Vicinity [EF3 COL 2.0-28-A]

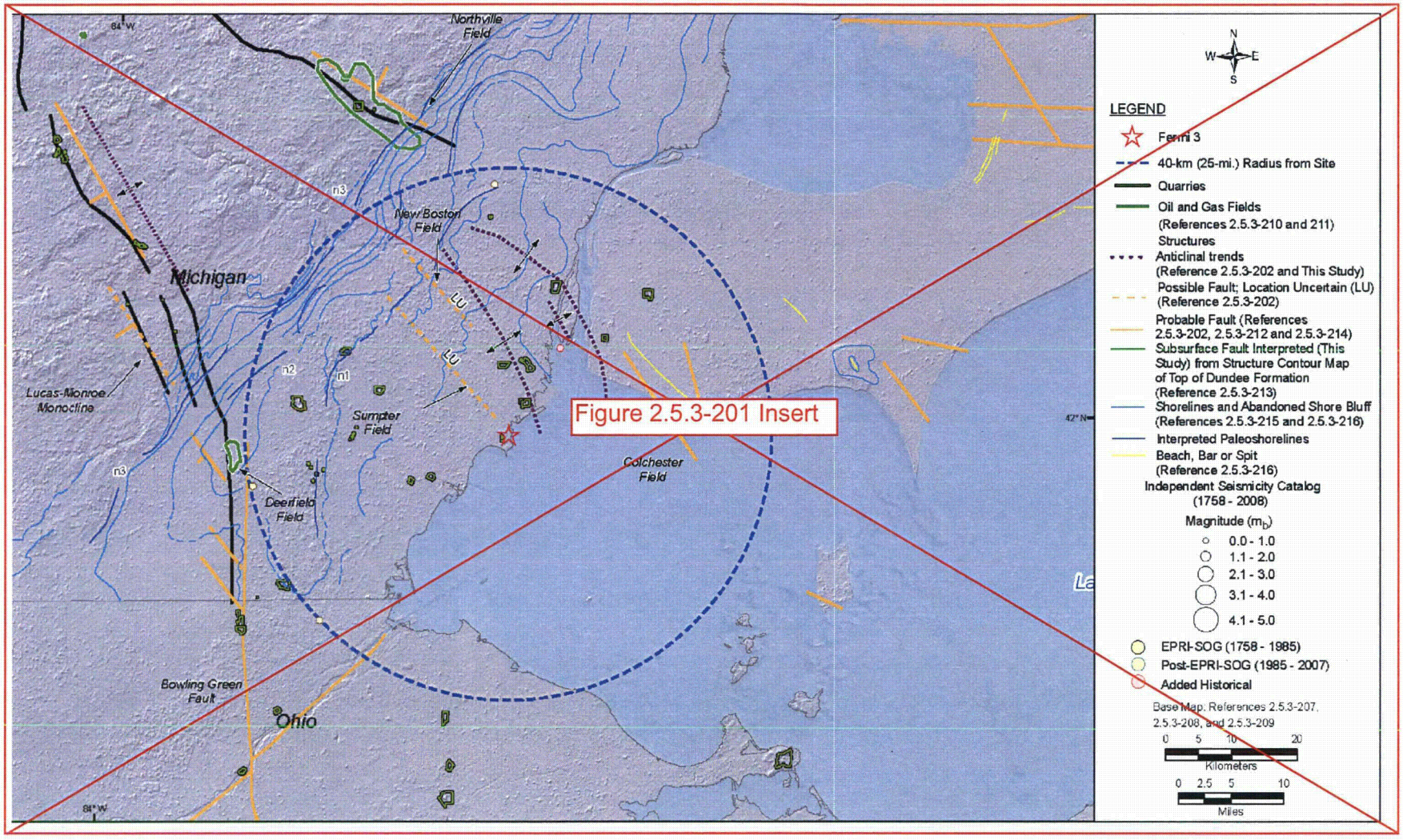

Figure 2.5.3-201 Insert

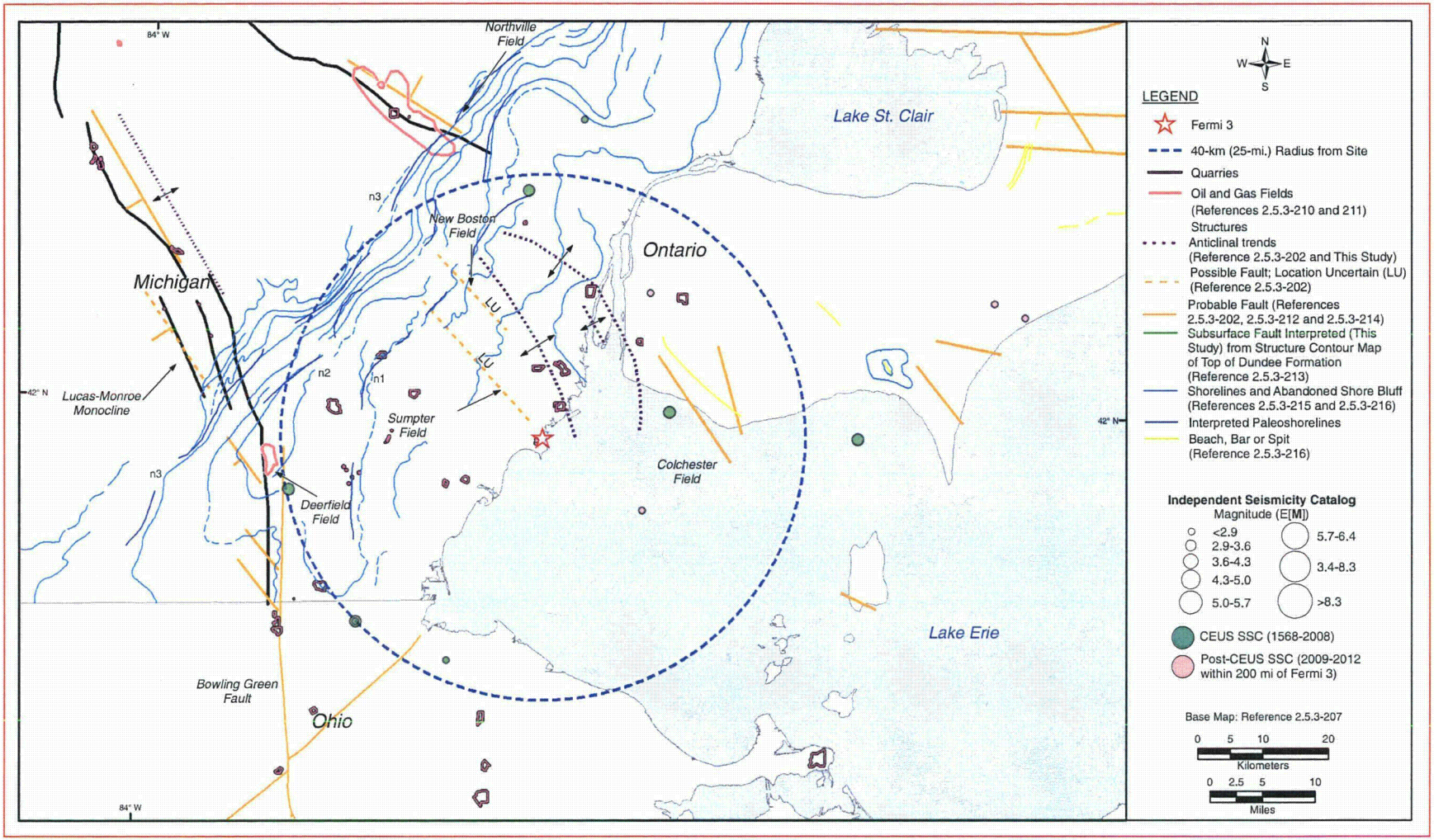

criterion is 29.3 and 31.0 degrees, respectively. The effective cohesion intercept, c', was neglected. Conservative estimates of the Mohr-Coulomb parameters with $\phi' = 29^{o}$ and c' = 0 are used for lacustrine deposits. Based on the pore pressure response of the lacustrine deposits from $\overline{CU}$ tests, lacustrine deposits are considered slightly overconsolidated soil.

Unit weight and moisture content were measured in the laboratory for lacustrine deposits. Average dry unit weight of the lacustrine deposits is approximately 16.5 kN/m^3 (105 pcf), with an average natural moisture content of 27 percent.

The lacustrine deposits are not considered suitable for foundation support or structural backfill for Fermi 3 due to low undrained shear strength. Lacustrine deposits material will be removed in the Fermi 3 area and consolidation characteristics of lacustrine clay are not needed.

The static engineering properties of lacustrine deposits presented herein are suitable for stability analysis and design of temporary excavation support systems and slopes, where applicable.

Since lacustrine deposits will be excavated in the Fermi 3 area and are not considered as competent material due low shear strength, the dynamic engineering properties of the lacustrine deposits are not needed for ground motion response analysis.

2.5.4.2.1.1.3 Glacial Till

A detailed description and classification of glacial till is provided in Subsection 2.5.1.2.3.2.3.1 Glacial till was encountered from approximately elevation 171.6 to 168.2 m (563 to 552 ft) NAVD 88. It is classified as lean with an average of 68 percent fines. The plasticity index of glacial till ranges from 7 to 27 percent, with an average of 14 percent. Its liquid limit ranges from 18 to 47 percent, with an average of 29 percent. In general, it is observed that the gravel content increases with increasing depth in the glacial till.

(elevation 552 ft rounded from 551.7 ft)

During the subsurface investigation at Fermi 3, 72 SPT were performed within the glacial till. In addition, laboratory tests were performed to characterize the properties of glacial till as discussed in Subsection 2.5.4.2.3. The results of the field and laboratory tests together with their variability are summarized in Table 2.5.4-204.

The average S_U measured from three UC and two UU tests is 124.5 and 76.6 kPa (2.6 and 1.6 ksf), respectively. In addition, the average S_U measured from three $\overline{CU}$ tests, isotropically consolidated to their in-situ vertical effective stress, is 167.6 kPa (3.5 ksf). Based on the above three methods, an average S_U of 129.3 kPa (2.7 ksf) was chosen for design.

Twelve $\overline{CU}$ tests were performed on the glacial till. The ϕ' and c' values, based on the maximum principal stress difference criteria, are 30.6 degrees and 0, respectively. The ϕ' and c' values, based on the peak principal stress ratio failure criterion, are 31.3 degrees and 14.4 kPa (0.30 ksf), respectively. In addition to the $\overline{CU}$ tests, a set of three direct shear tests was performed. The results indicated a ϕ' of 37 degrees and c' of approximately 0 for glacial till. Conservative estimates of the Mohr-Coulomb parameters, with $\phi' = 31^o$ and c' = 0 are used for glacial till. Based on the pore pressure response of glacial till from $\overline{CU}$ tests, the till is considered as heavily overconsolidated soil.

Unit weight and moisture content were measured in the laboratory for glacial till. Average dry unit weight of the till is approximately 17.9 kN/m^3 (114 pcf), with an average natural moisture content of 15 percent.

E was computed from plots of axial stress versus axial strain based on UU and $\overline{CU}$ laboratory tests results. The average calculated E is approximately 28.7 MN/m^2 (600 ksf).

The glacial till will be removed from under Seismic Category I structures. However, based on the characteristic of glacial till, it may be used to support Non-Seismic Category I structures.

The static engineering properties of glacial till presented herein are suitable for stability analysis and design of temporary excavation support systems and slopes, and foundation support, where applicable.

Subsection 2.5.4.4.1 discusses the techniques used to measure shear wave velocity (V_s) and compression wave velocity (V_p) and the results of the testing. The measured V_s ranges from 244 to 351 m/s (800 to 1,150 fps) based on the spectra analysis of surface waves (SASW) method. The measured V_s is used to calculate the low-strain shear modulus of glacial till. Subsection 2.5.4.7 discusses the shear modulus behavior at larger strain levels.

Based on static and dynamic engineering properties presented above, glacial till is considered as the upper most competent material at Fermi 3.

; however, the glacial till will be removed in the vicinity of Seismic Category I structures and is not considered in ground motion response analysis for Fermi 3 in Subsection 2.5.2.

~~The dynamic engineering properties of the till are suitable for ground motion response analysis for Fermi 3.~~

2.5.4.2.1.2 Engineering Properties of Bedrock

This section discusses the engineering properties of bedrock units encountered at Fermi 3 including Bass Islands Group, and Salina Group Units F, E, C and B. Seismic Category I structures at Fermi 3 are directly founded on the Bass Islands Group or on fill concrete overlying the Bass Islands Group.

A detailed description and classification of the Bass Islands Group is provided in Subsection 2.5.1.2.3.1.2. Subsection 2.5.1.2.3.1.1 presents a detailed description and classification of Salina Group Units F, E, C and B.

In each of the following sections, the properties of each bedrock unit based on field and laboratory testing results are presented with their variability. The strength and deformation characteristics of bedrock units were also estimated using Hoek-Brown criterion (Reference 2.5.4-201), which uses the following five input parameters to estimate rock mass strength:

1. q_u of intact rock core samples.
2. Material index (mi) related to rock mineralogy, cementation, and origin.
3. Geological strength index (GSI) that factors the intensity and surface characteristics of rock mass discontinuities.
4. Disturbance factor (D) related to the level of the rock mass disturbance due to construction excavation and blasting.
5. Laboratory measured E of the intact rock core samples.

The input parameters, for each bedrock unit, used to estimate rock mass strength based on Hoek-Brown criterion are summarized in Table 2.5.4-205.

Finally, measured mean V_s and V_p are presented based on the results presented in Subsection 2.5.4.4.1. Subsection 2.5.4.4.1 discusses the techniques used to measure V_s and V_p and the results of the testing.

- Direct shear tests on rock per ASTM D5607 (Reference 2.5.4-224)
- Hydraulic conductivity using a flexible wall permeameter per ASTM D5084 (Reference 2.5.4-225)
- Chemical analysis of soils per ASTM G51, ASTM D512 and ASTM D516 (Reference 2.5.4-226 through Reference 2.5.4-228)

The results for index properties, gradation and chemical analysis of soil samples are summarized in Table 2.5.4-220. Table 2.5.4-221 shows the results for strength tests of soil samples from $\overline{CU}$, UU and UC tests. The unconfined compressive strength tests and direct shear tests on discontinuities of rock core samples are summarized in Table 2.5.4-222 and Table 2.5.4-223, respectively.

The mean V_s for the Bass Islands Group, Salina Groups Units E, C and B were greater or equal to 2,042 m/s (6,700 fps) as shown in Table 2.5.4-202; therefore, no dynamic testing is required for these bedrock units. The need to perform dynamic testing was investigated for Salina Group Unit F, with a mean V_s ranging from 975 to 1,219 m/s (3,200 to 4,000 fps). It was concluded that no dynamic testing is required for this bedrock unit based on the following:

1. The shear strain that would be induced in Salina Group Unit F during the postulated design earthquake was estimated. The calculation was performed using the assumption of peak ground acceleration of 0.25 g and minimum V_s = 549 m/s (1,800 fps) measured at Boring TB-C5 at a depth of approximately 73.2 m (240 ft). The estimated shear strain would be approximately 0.0252 percent, which would indicate a ratio of G/G_{max} of approximately 0.91. To approximate a worst case, this G/G_{max} is based on sand between depths of 36.6 to 76.2 m (120 to 250 ft) (EPRI, 1993, Reference 2.5.4-229). The actual G/G_{max} for bedrock would be larger, indicating negligible modulus reduction for the bedrock. The statistics for the level of effective strain computed in the analyses for the 10^{-4} and 10^{-5} input ground motions are shown on Figure 2.5.2-271 and Figure 2.5.2-272, respectively. Figure 2.5.2-271 and Figure 2.5.2-272 show that within the elevation range of the Salina Group Unit F (elevations of approximately 103 to 141 m [339 to 462 ft]) the computed shear strains in the randomized site profiles were all less than or equal to 0.03 percent. Therefore, these results

280
281
281
280

Four Resonant Column and Torsional Shear (RCTS) tests are performed to establish the dynamic properties of the till. The RCTS testing provides the modulus reduction and damping of the glacial till as a function of strain up to shear strain of approximately 0.3 percent. RCTS test results are presented in Subsection 2.5.4.7.3.

confirm the estimated shear strain level in Salina Unit F is less than 0.03 percent.

2. Core recovery and RQD in Salina Group Unit F was poor. Testable samples from Salina Group Unit F were collected and preserved. These samples likely represent the more intact portions of the bedrock and hence testing under static or dynamic loading conditions would possibly give high values not representative of the overall Unit F.

~~Using an estimated average V_S of 305 m/s (1,000 fps) for till, the strain levels induced in till during the design earthquake was estimated to be 0.03 percent, with a resultant modulus reduction that would not exceed 20 percent. Therefore, only Resonant Column and Torsional Shear (RCTS) Testing is needed to obtain the dynamic response of the till. The RCTS testing will provide the dynamic response of soils up to shear strain of approximately 0.5 percent. No cyclic triaxial and cyclic direct simple shear tests are required. Figure 2.5.2-271 and Figure 2.5.2-272 show that within the elevation range of the glacial till (elevations of approximately 168 to 172 m [552 to 563 ft]) the computed shear strains in the randomized site profiles were all less than or equal to 0.1 percent. The RCTS testing provides the modulus reduction characteristic of glacial till up to shear strain of approximately 0.3 percent as shown on Figure 2.5.4-226. Therefore, these results confirm that cyclic triaxial and cyclic direct simple shear tests were not necessary since RCTS testing provides the modulus reduction characteristic for glacial till up to approximately 0.3 percent.~~

~~A number of dynamic tests on samples of glacial till to obtain the modulus reduction and damping curves as a function of strain were performed. Four RCTS tests were performed on glacial till as presented in Subsection 2.5.4.7.3.~~

2.5.4.3 Foundation Interface

Figure 2.5.1-236 shows the locations of the site explorations including borings, monitoring wells, piezometers and the test pit at Fermi 3 for the geotechnical investigation. Figure 2.5.4-201 shows the plan view of the excavation (discussed in Subsection 2.5.4.5) for the following ESBWR technology structures:

- Reactor Building/Fuel Building (RB/FB), Seismic Category I
- Control Building (CB), Seismic Category I

2.5.4.5.4.2 Backfill Materials and Quality Control

Backfill for Fermi 3 may consist of fill concrete or a sound, well graded engineered granular backfill. Subsection 3.7.2 presents the results of the Fermi 3 site-specific soil-structure interaction (SSI) analyses for the RB/FB and CB with fill concrete included as the backfill below the top of the Bass Islands Group bedrock, and engineered granular backfill above the top of the bedrock ~~neglected~~. The Fermi 3 site-specific SSI results show that, with the engineered granular backfill neglected, the RB/FB and CB are within the Referenced DCD structural design and stable against sliding and overturning, as discussed in Subsection 3.8.5. The soil-structure interaction analyses in the Referenced DCD for the FWSC were performed as a surface structure, so the backfill surrounding the FWSC foundation basemat is not included in the Referenced DCD SSI. The Referenced DCD sliding analysis considers the backfill supporting and surrounding the basemat. For the FWSC, the supporting material below the FWSC at Fermi 3 is fill concrete with a mean compressive strength of 31 MPa (4,500 psi) versus the soil with an angle of internal friction of 35 degrees used in the Referenced DCD. As discussed in Subsection 3.8.5, sliding of the FWSC is not an issue when neglecting the engineered granular backfill surrounding the basemat. Therefore, the engineered granular backfill surrounding the basemat for the FWSC is not Seismic Category I backfill.

with and without

The Fermi 3 engineered granular backfill surrounding the Seismic Category I structures will meet the following Referenced DCD requirements:

i. Product of peak ground acceleration α (in g), Poisson's ratio ν and density γ

   $\alpha(0.95\nu + 0.65)\gamma$: 1220 kg/m^3 (76 lbf/ft^3) maximum

ii. An angle of internal friction equal to or greater than 35 degrees when properly placed and compacted.

iii. Soil density

   γ: 2000 kg/m^3 (125 lbf/ft^3) minimum

The DCD requirement $\alpha(0.95\nu + 0.65)\gamma$ is retained because it is associated with the dynamic lateral earth pressure of the engineered granular backfill on the embedded walls of Seismic Category I RB/FB and CB. The DCD requirements for angle of internal friction and density are retained to ensure a dense backfill.

Evaluation and discussion of liquefaction issues related to soil backfill materials is provided in Subsection 2.5.4.8. Lateral pressures applied against foundation walls are evaluated and discussed in Subsection 2.5.4.10.

The gradation of the engineered granular backfill will be selected to approximate a hydraulic conductivity of 8.85 x 10^{-4} m/s (251 ft/day) (Subsection 2.4.12.2.4) or greater.

A quality control sampling and testing program is developed to verify that fill concrete and engineered granular backfill material properties conform to the specified design parameters. Sufficient laboratory compaction and grain size distribution tests are performed to account for variations in fill material. A test fill program may be included for the purposes of determining an optimum size of compaction equipment, number of passes, lift thickness, and other relevant data for achievement of the specified compaction.

Fill concrete used as fill under the FWSC, Seismic Category II structures, and surrounding the RB/FB and CB to the top of bedrock will be proportioned, tested and the placement controlled in accordance with Regulatory Guide 1.142. Additionally, ACI 349 requirements for concrete exposed to sulfate-containing solutions will be implemented. The fill concrete will have a mean 28-day compressive strength of equal to, or greater than, 31 MPa (4,500 psi) with a mean shear wave velocity of equal to, or greater than ~~1,100 m/s (3600 ft/s)~~ 2,175 m/s (7,140 ft/s). Compressive strength of the fill concrete will be tested in accordance with Regulatory Guide 1.142. The compressive strength of the fill concrete will be used to calculate shear wave velocity to ensure that the shear wave velocity of ~~1,100 m/s (3600 ft/s)~~ 2,175 m/s (7,140 ft/s) is met. The mix design developed for the fill concrete will control erosion and leaching due to contact with site groundwater and limit settlement to specified tolerances (Table 2.0-201), including creep and shrinkage.

The quality control program for fill concrete includes requirements for compressive strength testing. Verification will be performed to confirm that compressive strength testing results comply with mix design, minimum strengths, and placement requirements. The details of the quality control program will be addressed in a design specification prepared during the detailed design phase of the project.

2.5.4.7.5 Shear Modulus Reduction and Damping for Soils

No Seismic Category I structures are founded on soil. The RB/FB and CB are founded on bedrock. The FWSC is founded on fill concrete extending to bedrock. ~~The fill and lacustrine deposits are removed under all foundations in the power block area; therefore, no shear modulus and damping curves are presented for these materials.~~

Insert 8

~~The modulus reduction and damping curves for glacial till are needed for developing the GMRS. The shear modulus and damping curves for glacial till are chosen from published correlations (Reference 2.5.4 229). As shown in Table 2.5.4 204, the plasticity index of glacial till ranged from 7 to 27 percent with a mean value of 14 percent. The shear modulus reduction and damping curves with plasticity index equal to 15 and 50 were selected for glacial till as discussed in Subsection 2.5.2.5.1.2. The modulus reduction and damping curves were then randomized as shown on Figure 2.5.2 259 and Figure 2.5.2 260 as discussed in Subsection 2.5.2.5.1.3.~~

~~Measured shear modulus reduction and damping data from RCTS testing and published curves for a range of plasticity index values are plotted for comparison on Figure 2.5.4 226. The measured modulus reduction and damping curves from the RCTS tests are well within the randomized plasticity index 15 and 50 curves as shown on Figure 2.5.2 259 and Figure 2.5.2 260.~~

2.5.4.7.6 Shear Modulus Reduction and Damping Curves for Granular Backfill and Fill Concrete

Engineered granular backfill is not used to support any Seismic Category I structures. Engineered granular backfill is mainly used as backfill surrounding the embedded walls of structures or to backfill beneath other structures with foundation levels above bedrock, except Seismic Category II structures, which are founded on fill concrete.

The shear modulus and damping ~~curves~~ for engineered granular backfill are discussed in Subsection 3.7.1.1.4.1.1.

and fill concrete

~~Shear modulus reduction and damping curves for assumed lean concrete fill using a lower bound compressive strength of 2.1 MPa (300 psi) used for site response analysis are discussed in Subsection 2.5.2.5.~~

Insert 8

The fill, lacustrine deposits, and glacial till are removed in the vicinity of Seismic Category I structures; therefore, no shear modulus and damping curves are required for these materials.

For the glacial till, RCTS testing is performed to provide measured shear modulus reduction and damping data. Table 2.5.4-204 shows that the plasticity index (PI) of the glacial till ranges from 7 to 27 percent, with a mean value of 14 percent. The glacial till shear modulus reduction and damping data are plotted on Figure 2.5.4-226 along with modulus reduction and damping relationships developed by Vucetic and Dobry (Reference 2.5.4-255) for clays with PI values of 15, 30, 50, and 100 percent. The measured shear modulus reduction and damping values from the RCTS tests are generally within the relationships developed by Vucetic and Dobry (Reference 2.5.4-255) for clays with PI values of 15, 30, and 50 percent.

2.5.4.7.7 Ground Motion Response Spectra

The seismic velocity profiles are shown on Figure 2.5.4-220 through Figure 2.5.4-225. The GMRS ~~and FIRS~~ based on these velocity profiles ~~and modulus reduction and damping curves are~~ is described in Subsection 2.5.2.6. The Foundation Input Response Spectra (FIRS) for the RB/FB, CB, and FWSC are discussed in Subsection 3.7.1.

2.5.4.8 Liquefaction Potential

This section conforms to guidelines in RG 1.198.

All Seismic Category I structures are supported within the Bass Islands dolomite or on fill concrete extending to the top of bedrock. Neither the bedrock nor fill concrete are susceptible to liquefaction.

For engineered granular backfill adjacent to Seismic Category I structures, liquefaction considerations only apply below the groundwater table. Subsection 2.4.12.5 provides the maximum historical high groundwater level elevation of 175.6 m (576.11 ft) NAVD 88, which is approximately 4 m (13.2 ft) below the plant grade elevation of 179.6 m (589.3 ft) NAVD 88; therefore, liquefaction is not a consideration in the upper 4 m (13.2 ft) of the engineered granular backfill. Subsection 2.5.4.5.4.2 discusses placement of granular backfill adjacent to Seismic Category I structures in controlled lifts with compaction. This will result in a dense to very dense consistency engineered backfill surrounding the embedded walls of Seismic Category I structures; therefore, there is also no potential for liquefaction in the engineered granular backfill below the groundwater. For confirmation, a liquefaction analysis based on the SPT is provided to demonstrate that the engineered granular backfill is not susceptible to liquefaction.

Reference 2.5.4-251, Table 12.1 shows that for dense granular soils N_{60} is between 30 and 50 blows/foot, and for very dense granular soils N_{60} is greater than 50 blows/foot. N_{60} is the numbers of blows to drive a standard split barrel sampler the last 12 inches of the SPT using a 140 pound hammer falling 30 inches, where the hammer has a 60 percent energy efficiency. To evaluate liquefaction potential of soil, $(N_1)_{60}$ is needed, where $(N_1)_{60}$ is the N_{60} value normalized to an overburden pressure of approximately 100 kPa (1 ton per square foot) (Reference 2.5.4-252). Reference 2.5.4-252 shows that for historical data, no liquefaction was observed when $(N_1)_{60}$ is greater than 30 blows/ft.

For the engineered granular backfill, the N_{60}-value is estimated to be 30 blows/foot at the ground surface, and is increased linearly to 60

blows/foot at a depth of 65 feet. Using this distribution for N_{60} and a bounding groundwater level at 2 feet below finished ground level grade, at all engineered granular backfill depths for the full depth of the deepest Seismic Category I structure, $(N_1)_{60}$ is greater than 30 blows/foot. With the backfill placement approach and resultant $(N_1)_{60}$ greater than 30, it is concluded that the engineered granular backfill, adjacent to all Seismic Category I structures, is not susceptible to liquefaction. If $(N_1)_{60}$ of the in-place engineered granular backfill is less than 30, a more refined liquefaction analysis will be performed to confirm there is adequate resistance against liquefaction.

Backfill below Seismic Category II structures from the base of the foundation to the top of bedrock is fill concrete; therefore, liquefaction analysis for soil below Seismic Category II structures is also not necessary.

The existing fill, lacustrine deposits and glacial till are removed under and adjacent to all Seismic Category I structures; therefore, liquefaction analysis for these soils is not necessary.

Glacial till and/or engineered granular backfill ~~will~~ can be used as foundation support under non-Category I and II structures that ~~could~~ can not strike a Seismic Category I structure if it were to fail during a seismic event. Glacial till is not susceptible to liquefaction based on its USCS classification as lean clay (CL) and fines content greater than 30 percent (Table 2.5.4-202). As described above, engineered granular backfill is not susceptible to liquefaction.

2.5.4.9 Earthquake Design Basis

The V_s values of soils and bedrock at the site were determined through the field exploration program using geophysical testing as described in Subsection 2.5.4.2 and Subsection 2.5.4.4. Subsection 2.5.4.7 presents the dynamic response of soil and bedrock under dynamic loading conditions. The top of generic bedrock is approximately 129.5 m (425 ft) below the existing ground surface where the V_s of bedrock (Salina Group Unit B) is greater than 2804 m/s (9200 fps). A site response analysis was performed using the above information to develop the GMRS for the site as described in Subsection 2.5.2.6.

2.5.4.10 Static Stability

In this section, the analyses performed to evaluate the stability of the safety-related structures under static loading conditions are presented. Specifically, this subsection addresses three Seismic Category I structures – RB/FB, CB and FWSC. This section includes analyses of foundation bearing capacity and settlement, excavation rebound, lateral earth pressures, and hydrostatic pressures.

psf) compactive surcharge pressure is appropriate for the additional compaction lateral earth pressures that are developed (Reference 2.5.4-245).

2.5.4.10.3.1 Static Lateral Earth Pressures

The at-rest static lateral earth pressure σ_h for a given depth z is calculated as follows (Reference 2.5.4-246):

$$\sigma_h = K_0\sigma_0^{'} + u \qquad \text{[Eq. 8]}$$

where:

K_0 = coefficient of at-rest earth pressure = $1-\sin\phi$

u = pore water pressure

$\sigma_0^{'}$ = effective vertical subsurface stress = $q+\gamma z$ (q is surcharge load, γ is effective soil unit weight)

ϕ = angle of internal friction = 35 degree

2.5.4.10.3.2 Dynamic Lateral Earth Pressures

Insert 9 →

~~A method developed by Ostadan is used to compute seismic soil pressure on building walls (Reference 2.5.4-247). The peak response horizontal ground acceleration was used for the analyses of the seismic lateral earth pressure on the RB/FB and CB walls. The peak response horizontal ground acceleration is approximately 0.50g for both the RB/FB and CB based on site specific FIRS as shown on Figure 2.5.2-289 and Figure 2.5.2-290.~~

~~2.5.4.10.3.3 Results of Lateral Earth Pressure Analyses~~

~~The results of the static soil lateral earth pressure and seismic soil lateral earth pressure for the RB/FB and CB are shown on Figure 2.5.4-229 and Figure 2.5.4-230, respectively.~~

2.5.4.11 Design Criteria

DCD Table 2.0-1 shows the envelope of ESBWR standard site parameters. Subsection 2.5.4 addresses specifically the following parameters listed in DCD Table 2.0-1:

- Minimum Static Bearing Capacity.
- Minimum Dynamic Bearing Capacity.

Insert 9

A method developed by Ostadan and White (Reference 2.5.4-247) and a method presented in ASCE 4 (Reference 2.5.4-256) are both used to compute seismic lateral earth pressure on RB/FB and CB embedded walls. For the Ostadan and White method, the peak response horizontal ground acceleration of approximately 0.58g is selected for the RB/FB and CB based on site-specific FIRS shown on Figure 3.7.1-228 and Figure 3.7.1-229, respectively. Thirty percent damping is applied when using the Ostadan and White method; however, SRP 3.7.2 limits the composite modal damping to a maximum of 20 percent. Therefore, the peak horizontal ground accelerations from Figure 3.7.1-228 and Figure 3.7.1-229 are modified using a factor of 0.7 based on Reference 2.5.4-257 for a ratio of 20 to 5 percent damping. Application of this correction results in a peak response horizontal ground acceleration of approximately 0.41g used with the Ostadan and White method for both the RB/FB and CB.

The ASCE 4 method uses the peak ground acceleration of 0.2368g at the finished ground level grade from Table 3.7.1-205 to compute seismic lateral earth pressure on RB/FB and CB embedded walls.

For both methods, the engineered granular backfill is considered to extend the full depth of the RB/FB and CB; however, below the top of the Bass Islands Group bedrock the excavations will be backfilled with fill concrete. Once cured, the fill concrete will not apply lateral pressure to the RB/FB or CB; therefore, the engineered granular backfill lateral earth pressures estimates are bounding, as they are greater than will occur.

2.5.4.10.3.3 Results of Lateral Earth Pressure Analyses

For the RB/FB and CB, the results of the static lateral earth pressure and seismic lateral earth pressure using both the Ostadan and White, and ASCE 4 methodologies are shown on Figure 2.5.4-229 and Figure 2.5.4-230. The results of the Ostadan and White method are generally greater than the ASCE 4-98 method, since a higher acceleration is used with the Ostadan and White method.

- Minimum Shear Wave Velocity.
- Liquefaction Potential.
- Angle of Internal Friction.
- Maximum Settlement Values for Seismic Category I Buildings.

The design criteria required for minimum static and dynamic bearing capacity is addressed in Subsection 2.5.4.10.1. The factor of safety for static bearing capacity is at least 3 while for the dynamic bearing capacity is at least 2.25. The selection of shear strength parameters used in the bearing capacity evaluation is discussed in Subsection 2.5.4.2.1.

Results of the geophysical surveys for shear wave velocity are presented in Subsection 2.5.4.4.1 and shear wave velocity profiles are summarized in Subsection 2.5.4.7.2. The minimum shear wave velocity of the supporting foundation material associated with seismic strains for lower bound soil properties at minus one sigma from the mean is greater than 300 m/s (1,000 fps) as discussed in Subsection 2.5.4.7.2. Fill concrete is used as the backfill surrounding RB/FB and CB embedded walls below the top of bedrock and below the FWSC. Fill concrete meets the shear wave velocity requirement. For backfill above the top of the bedrock surrounding Seismic Category I embedded walls, the Fermi 3 site-specific soil-structure interaction analyses (Subsection 3.7.2) show that the Referenced DCD requirements for backfill surrounding Seismic Category I RB/FB and CB are not required.

Bass Islands Group

For the FWSC, the supporting material below the FWSC at Fermi 3 is fill concrete with a mean compressive strength of 31 MPa (4,500 psi) with 3000 mm (9.8 foot) deep shear keys extending into the fill concrete; therefore, sliding of the FWSC is not an issue as discussed in Subsection 3.8.5 when neglecting the engineered granular backfill surrounding the basemat. Therefore, the Referenced DCD requirements for backfill surrounding FWSC are not required.

The static stability analyses are presented in Subsection 2.5.4.10. The design criteria for static stability analyses are identified in Subsection 2.5.4.10 and are compared to site parameters in Table 2.0-201. Discussion of the assumptions and methods of analyses for the static stability analyses are provided in Subsection 2.5.4.10.

Subsection 2.5.4.8 discusses the liquefaction potential of soils encountered and fill at the site. It is concluded that there are no liquefiable soils under and adjacent to all Seismic Category I structures.

2.5.4-244 Peck, R.B., W.E. Hanson, and T. H. Thornburn, "Foundation Engineering," 2nd edition., Wiley and Sons, New York, 1974.

2.5.4-245 Black & Veatch, "Guide for Lateral Earth Pressure," Guide number: Energy-Gid-3-03112-03130, Revision 2, January 12, 2007.

2.5.4-246 Das, B. M., "Principles of Foundation Engineering," 5th Edition, Brooks/Cole- Thomson Learning, Pacific Grove, CA, 2004.

2.5.4-247 Ostadan, F., and W. H. White, "Lateral Seismic Soil Pressure: An Updated Approach," Proceedings of U.S.-Japan SSI Workshop, Menlo Park, CA, 1998.

2.5.4-248 Borehole and Surface Geophysics Boreholes CB-C3, RB-C4, RB-C8, RB-C6, and TB-C5 Surface Arrays near RW-C1, RB-C4, MW-393 and MW-381. GEOVision Report, 7297-01 Rev 0.

2.5.4-249 Black & Veatch, ARM Project No.: 07274, Geophysical Well Logging DTE Fermi 3 COL Monroe, Michigan, June 8, 2008.

2.5.4-250 Letter from GRL Dynamic Measurement and Analysis, Standard Penetration Test (SPT) Energy Measurements, July 2, 2007

2.5.4-251 Terzaghi, K., R.B. Peck, and G. Mesri, "Soil Mechanics in Engineering Practice," Third Edition, John Wiley & Sons, Inc., 1996.

2.5.4-252 Youd, T.L., et al., Liquefaction Resistance of Soils: Summary Report from the 1996 NCEER and 1998 NCEER/NSF Workshops on Evaluation of Liquefaction Resistance of Soils, Journal of the Geotechnical and Geoenvironmental Engineering, Vol. 127, No.10, pp. 817-833, ASCE, 2001.

2.5.4-253 ASTM C1260-07, "Standard Test Method for Potential Alkali Reactivity of Aggregates (Mortar-Bar Method)"

2.5.4-254 ASTM C1293-08b, "Standard Test Method for Determination of Length Change of Concrete Due to Alkali-Silica Reaction"

Insert 10 →

Insert 10

2.5.4-255 Vucetic, M., and R. Dobry, "Effect of Soils Plasticity on Cyclic Response," *Journal of Geotechnical Engineering,* American Society of Civil Engineers, Vol. 117, No. 1, 1991.

2.5.4-256 American Society of Civil Engineers 4-98, "Seismic Analysis of Safety-Related Nuclear Structures and Commentary"

2.5.4-257 Cameron, W.I. and Green, R.G., "Damping Correction Factors for Horizontal Ground-Motion Response Spectra," Bulletin of the Seismological Society of America, Vol. 97, No. 3, pp 934-960, June 2007.